9

Research Article

Chuangmin Li, Lubiao Liu, Youwei Gan*, Qinhao Deng, and Shuaibing Yi

Investigating the anti-aging properties of asphalt modified with polyphosphoric acid and tire pyrolysis oil

https://doi.org/10.1515/rams-2024-0017 received September 21, 2023; accepted April 15, 2024

Abstract: This research focuses on the aging resistance properties of asphalt, which are crucial for determining the lifespan of asphalt pavement. To combat aging, waste tire pyrolysis oil (TPO) is often added to asphalt, enhancing its resistance to aging but compromising high-temperature performance. This study offered a pioneering solution by integrating TPO with polyphosphoric acid (PPA) to address these issues. In this study, we conducted a series of tests to characterize the properties of PPA/TPO modified asphalt, including temperature sweep and bending beam rheometer tests. The results demonstrated that the presence of PPA in the PPA/TPO modified asphalt could improve its high-temperature performance while maintaining its low-temperature

properties. Moreover, PPA in the PPA/TPO modified asphalt enhanced the modified asphalt's resistance to fatigue and deformation during the aging process, while the presence of TPO effectively reduced the impact of thermo-oxidative aging on the modified asphalt during the aging process. Additionally, physicochemical interactions between the base asphalt and modifiers were observed before and after aging. In summary, this study had offered an innovative method to enhance the anti-aging properties of asphalt, and had provided more options for sustainable, environmentally friendly roads.

Keywords: modified asphalt, tire pyrolysis oil, polyphosphoric acid, asphalt aging characteristics, high-temperature rheological properties

* Corresponding author: Youwei Gan, School of Traffic and Transportation Engineering, Changsha University of Science and Technology, Changsha 410114, Hunan, China; Key Laboratory of Road Structure and Material of Ministry of Transport (Changsha), Changsha University of Science & Technology, Changsha 410114, Hunan, China, e-mail: ganyouwei@stu.csust.edu.cn

Chuangmin Li: School of Traffic and Transportation Engineering, Changsha University of Science and Technology, Changsha 410114, Hunan, China; Key Laboratory of Road Structure and Material of Ministry of Transport (Changsha), Changsha University of Science & Technology, Changsha 410114, Hunan, China, e-mail: lichuangmin@csust.edu.cn Lubiao Liu: School of Traffic and Transportation Engineering, Changsha University of Science and Technology, Changsha 410114, Hunan, China; Key Laboratory of Road Structure and Material of Ministry of Transport (Changsha), Changsha University of Science & Technology, Changsha 410114, Hunan, China, e-mail: lubiaoliu@stu.csust.edu.cn Qinhao Deng: School of Traffic and Transportation Engineering, Changsha University of Science and Technology, Changsha 410114,

Changsha University of Science and Technology, Changsha 410114, Hunan, China; Key Laboratory of Road Structure and Material of Ministry of Transport (Changsha), Changsha University of Science & Technology, Changsha 410114, Hunan, China, e-mail: dqhMR1.645@stu.csust.edu.cn Shuaibing Yi: School of Traffic and Transportation Engineering, Changsha University of Science and Technology, Changsha 410114, Hunan, China; Key Laboratory of Road Structure and Material of Ministry of Transport (Changsha), Changsha University of Science & Technology, Changsha 410114, Hunan, China, e-mail: xiaoyi@stu.csust.edu.cn

1 Introduction

In the field of road construction, asphalt becomes the predominant pavement material. During their operational period, asphalt pavements undergo aging due to exposure to heat, oxygen, light, and water [1]. This aging process diminishes the stiffness and crack resistance of the asphalt mixtures, resulting in degraded pavement performance, shorter lifespan, and higher maintenance costs [2]. The aging of asphalt materials is a significant cause of pavement distress. Therefore, improving the anti-aging capabilities of asphalt materials is paramount for both extending road service life and reducing maintenance costs.

By 2030, it is estimated that 1.2 billion waste tires will have been generated worldwide [3]. Disposing of such a monumental number of waste tires haphazardly, either by random stacking or landfilling, not only results in substantial land resource wastage but also poses significant environmental hazards [4,5]. Waste tires are commonly utilized for retreading, as fuel, for recycling, and pyrolysis. Pyrolysis is considered among the most environmentally friendly methods compared to other waste tire treatment approaches [6]. Pyrolysis, a process involving the thermal

decomposition of waste tires at high temperatures under anaerobic conditions, yields 40% tire pyrolysis oil (TPO), 35% solid carbon black, 13% flammable gas, and 12% steel wire [7]. TPO, mainly composed of methyl- and ethyl benzene, limonene, and dimethylcyclohexene, has yet to find widespread usage, owing to its inferior combustion performance and high impurity content [8,9].

With the ongoing exploration of environmentally friendly road construction materials, researchers have discovered that TPO can serve as a rejuvenating agent in the preparation of microcapsules, improving the self-healing properties of asphalt binders [10]. Additionally, TPO also has acted as an anti-aging agent for asphalt, boosting its durability while lessening the stiffness typically associated with aging [11]. Further research has revealed that a combination of TPO and waste ethylene-propylene-diene-monomer (EPDM) rubber improves asphalt modification more than TPO alone. This approach not only addresses the poor storage stability of the EPDM rubber but also markedly improves the aging resistance and fatigue resistance of the asphalt binder [12-14]. However, while the inclusion of TPO imparts remarkable anti-aging properties to asphalt, an excessive amount of TPO can compromise its hightemperature performance. This stands as one of the major hindrances to TPO's widespread application and use in asphalt modifications [15]. While current researchers have attempted to enhance the high-temperature performance of TPO-modified asphalt by incorporating pyrolysis carbon black and crude palm oil, their studies do not primarily focus on the anti-aging properties of the asphalt binder [7,16]. Consequently, a key challenge for road research practitioners is to ensure the high-temperature performance of TPO-modified asphalt without compromising its anti-aging properties, to promote its widespread use in road modifications.

Polyphosphoric acid (PPA) is a commonly used asphalt modifier that can improve the high-temperature performance of asphalt binders by reacting with asphalt to create a more complex macromolecular structure [17]. For instance, research conducted by Liu et al. has demonstrated that in the case of PPA/waste engine oil modified asphalt, the presence of PPA can mitigate the adverse effects of waste engine oil on the high-temperature performance of the asphalt binder. Additionally, a 1-2% PPA content positively correlates with improved high-temperature performance in asphalt binders [18]. Meanwhile, Han et al. have found that certain amounts of PPA enhance rubber-modified asphalt's storage stability. However, the addition of an excessive amount of PPA leads to an excessive increase in the asphaltenes content within the rubber-modified asphalt, consequently impairing its storage stability [19]. However, what is more noteworthy is PPA's influence on the anti-aging performance of asphalt binders.

For instance, Liu *et al.* discovered that PPA can effectively enhance the short-term anti-aging ability of modified asphalt [20]. Based on these findings, it is hypothesized that employing PPA potentially enhances the high-temperature performance and anti-aging properties of TPO modified asphalt, a conjecture grounded in the aforementioned empirical evidence.

Asphalt aging is primarily due to thermal oxidation. Under laboratory conditions, the rolling thin-film oven test (RTFOT) and the pressure aging vessel (PAV) test can simulate both short-term and long-term asphalt aging. When equipment is limited or variables need to be controlled, RTFOT replaces PAV for long-term aging simulation by adjusting certain conditions like extending the aging time [21]. Furthermore, de Oliveira *et al.*'s research has indicated that the time equivalency between RTFO and PAV is about 255–340 min. This suggests that asphalt samples aged in the RTFO for 255–340 min approximate those aged under standard PAV conditions [22].

From a comprehensive analysis of existing literature, it becomes evident that extensive research indicates that utilizing TPO can compromise the high-temperature performance of modified asphalt, despite its potential to enhance resistance to aging. On the other hand, the introduction of PPA is recognized as amplifying the high-temperature stability of modified asphalt. However, a conspicuous gap remains in the literature regarding the simultaneous application of PPA and TPO in asphalt modification, and their combined effects on the high-temperature and anti-aging attributes of asphalt. The aim of this study is to carefully examine the high-temperature performance of asphalt modified with a PPA/TPO composite, and to elucidate the implications of incorporating PPA/TPO in the aging resistance of asphalt binders.

To achieve the objectives of this study, a series of asphalt binder specimens were created to represent different levels of aging by adjusting the duration of RTFOT. Subsequently, the high-temperature rheological properties of the asphalt binders were methodically evaluated using temperature sweep tests. In order to gain a deeper understanding of the aging resistance and fatigue characteristics during the asphalt aging stage, a linear amplitude sweep (LAS) test was conducted. Additionally, the influence of modifiers on the creep recovery capability and low-temperature crack resistance of asphalt binders was characterized using multiple stress creep recovery (MSCR) and bending beam rheometer (BBR) tests. Moreover, this study employed Fourier transform infrared (FTIR) spectroscopy and fluorescence microscopy tests to investigate the physicochemical effects of aging on asphalt binders and to clarify how modifiers physicochemically interact with the base asphalt.

2 Materials and methods

2.1 Raw materials

The study utilized base asphalt, specifically grade 70#, as per the test methodology outlined in ITG E20 [23], with the results of its properties documented in Table 1. TPO and PPA were procured from Hunan Qidi Environmental Technology Co., Ltd and Shanghai Aladdin Biochemical Technology Co., Ltd, respectively. The fundamental properties of each, as provided by the manufacturers, are detailed in Tables 2 and 3. In normal atmospheric conditions, PPA appeared as a colorless and transparent liquid, while TPO appeared as an oil-like liquid of brown or black hue. Figure 1 exhibits the macroscopic appearance of both modifiers.

2.2 Preparation of original composite asphalt

In order to investigate the impact of increasing the content of PPA and TPO additives on the performance of asphalt binders, and to consider the adverse effects of excessive TPO addition on asphalt binder properties, this study, through preliminary research and pre-trials, selected and prepared three types of modified asphalt with different modifier contents [18,24]. These three dosages were: 1% PPA and 4% TPO of the base asphalt mass ratio (referred to as 1/4), 2% PPA and 4% TPO of the base asphalt mass ratio (referred to as 2/4), 2% PPA and 6% TPO of the base asphalt mass ratio (referred to as 2/6). Initially, to ensure that the base asphalt achieved a fully fluid state, the base asphalt was heated to 135°C using an oven. Subsequently, various mass ratios of TPO and PPA were incorporated into the base asphalt, and the mixture was then blended using a Yixuan brand GS-1 type high-speed asphalt shearing machine. The blending was conducted at 135°C at a speed of 4,500 rpm for a duration of 45 min. This process resulted in the creation

Table 2: Fundamental properties of TPO

Index	Unit	Test results	Test method
Density (20°C)	kg·m ^{−3}	923	ISO 12185:1996
Moisture	%	0.1	ISO 3733:1999
Impurity	%	0.0017	ISO 10307:2009

Table 3: Fundamental properties of PPA

Assay (AS-	Assay	Density	Boiling
H ₃ PO ₄) (%)	(P ₂ O ₅) (%)	(25°C) (g·cm ⁻³)	point (°C)
≥116.77	94	2.06	300



Figure 1: Macroscopic morphology of raw materials: (a) PPA and (b) TPO.

of three different types of modified asphalt samples with varying concentrations of additives (notated as 0 min).

2.3 Preparation of the aged composite asphalt

To study the impact of aging time on the properties of modified asphalt, this study introduced composite asphalt at two distinct stages of aging. These were the composite asphalt subjected to 85 min of RTFOT to simulate short-

Table 1: Fundamental properties of base asphalt

Index	Unit	Test results	Test method
Penetration (25°C, 100 g, 5 s)	0.1 mm	78	T0604
Ductility (10°C, 5 cm·min ⁻¹)	cm	37.5	T0605
Softening point ($T_{R\&B}$)	°C	46	T0606
Index	After RTFOT		
Loss of quality	%	+0.5	T0610
Residual penetration ratio (25°C)	%	60	T0604
Residual ductility (10°C)	cm	11	T0605

term aging (referred to as 85 min), and the composite asphalt subjected to 270 min of RTFOT aging to simulate long-term aging (referred to as 270 min) [22]. The RTFOT aging conditions adhered to the specifications of T 0610-2011 [23]. The procedure involved placing 35 g asphalt in a standard sample bottle, then placing it in a preheated rotating oven. The aging process occurred under specific conditions, with an airflow rate of $4,000 \pm 200 \, \text{mL} \cdot \text{min}^{-1}$ and a temperature of $163 \pm 0.5 \,^{\circ}\text{C}$. The preparation process is illustrated in Figure 2.

2.4 Temperature sweep tests

The high-temperature performance of asphalt under various aging conditions was assessed by conducting temperature sweep tests with a dynamic shear rheometer (DSR). Specifically, the tests were performed using an MCR302 DSR, manufactured by Anton Paar, Austria. The temperature testing range was 58–84°C, in increments of 6°C per step. The test samples were 25 mm in diameter and 1 mm thick, with frequencies and strain levels set at 10 rad·s⁻¹ and 0.5%, respectively.

2.5 LAS tests

To evaluate the fatigue resistance of aged asphalt, the LAS test with a DSR, using the method described in AASHTO TP-101-16. Conducted at 25°C, the test specimen had a diameter of 8 mm and a thickness of 2 mm. Initially, a frequency sweep was carried out at 0.2–30 Hz under the same temperature, applying a 1% strain to identify the undamaged material parameters. The LAS test was subsequently conducted at the

same temperature, maintaining a constant sweep frequency of 10 Hz and varying the amplitude from 0.1 to 30% over a duration of 310 s. After the conclusion of the LAS test, the fatigue performance of the asphalt binder was evaluated. In accordance with AASHTO T 391-20, the frequency sweep test and LAS test results were analyzed and calculated using the viscoelastic continuum damage (VECD) theory. In this study, the asphalt's damage accumulation, denoted as D(t), and the fatigue performance parameter, indicated by $N_{\rm f}$, were represented by Eqs. (1) and (5), respectively.

$$D(t) \approx \sum_{i=1}^{N} [\pi I_{D} \gamma_{0}^{2} (|G^{*}| \sin \delta_{i-1} - |G^{*}| \sin \delta_{i})]^{\frac{a}{1+a}} (t_{i} - t_{i-1})^{\frac{1}{1+a}},$$
(1)

where $I_{\rm D}$ represents the initial value of $|G^*|$, measured at the 1% strain interval, in MPa. γ_0 denotes the applied strain, expressed as a percentage. G^* is the complex shear modulus, also measured in MPa, while t represents the duration in seconds. The value of parameter a is reported in Eq. (2).

$$a = 1 + \frac{1}{m},\tag{2}$$

where the parameter m is determined by simultaneously fitting both Eqs. (3) and (4).

$$G'(\omega) = |G^*|(\omega) \times \cos \delta(\omega),$$
 (3)

$$\log G'(\omega) = m(\log \omega) + b. \tag{4}$$

where $G'(\omega)$ represents the energy storage modulus derived from the dynamic modulus; $|G^*|(\omega)$ corresponds to each frequency during frequency sweep; and $\cos \delta(\omega)$ denotes the phase angle associated with each frequency.

$$N_{\rm f} = A_{35} (\gamma_{\rm max})^{-B}$$
, (5)

where the parameter A_{35} is derived from Eq. (6); $\gamma_{\rm max}$ represents the maximum expected strain in the pavement structure, expressed as a percentage; the constant B is defined as twice the value of a.

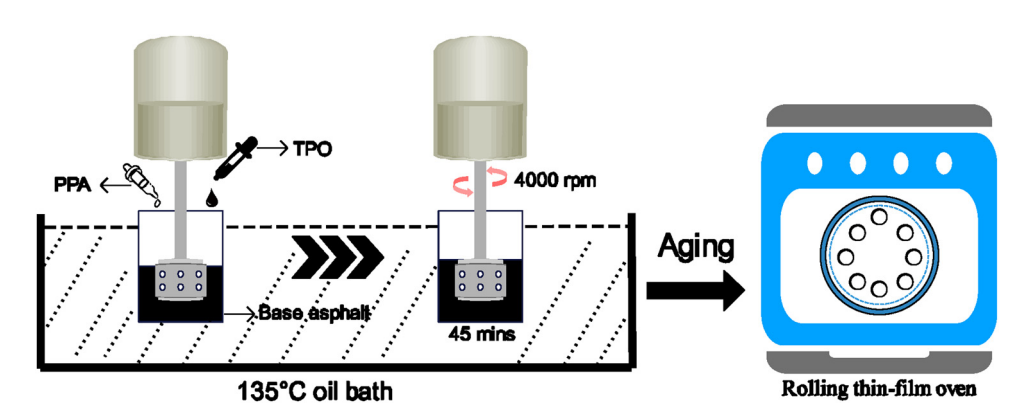


Figure 2: Preparation process of original composite asphalt and aged composite asphalt.

$$A_{35} = \frac{f(D_{\rm f})^k}{k(\pi I_{\rm D}C_1C_2)^a},\tag{6}$$

where f represents the load frequency, set at 10 Hz.; k is defined as $k = 1 + (1 - C_2)a$; C_1 and C_2 are parameters derived from linear fitting, as per Eq. (7); the term $D_{\rm f}$ denotes the failure damage, which is calculated using Eq. (8).

$$\log(C_0 - |G^*| \cdot \sin \delta) = \log(C_1) + C_2 \cdot \log(D), \tag{7}$$

where C_0 is the average value of $|G^*| \cdot \sin \delta$ at 0.1% strain interval.

$$D_{\rm f} = (0.35) \left(\frac{C_0}{C_1} \right)^{\left(\frac{1}{C_2} \right)}. \tag{8}$$

For each data point corresponding to Eq. (1), D(t) must also satisfy the relationship outlined in Eq. (9) with $|G^*| \cdot \sin \delta$.

$$|G^*| \cdot \sin \delta = C_0 - C_1(D)^{C_2}. \tag{9}$$

2.6 MSCR tests

To evaluate the asphalt's creep recovery ability under varying aging conditions after exposure to stress, MSCR tests were conducted using a DSR. Testing followed the AASHTO T 350-14 guidelines, utilizing the MCR302 DSR manufactured by Anton Paar, Austria, as the equipment. Tests were conducted at three temperatures: 58, 64, and 70°C. Samples measuring 25 mm in diameter and 1 mm in thickness were used. The procedure included two stresscontrolled modes at stress levels of 0.1 and 3.2 kPa.

2.7 BBR tests

To characterize the low-temperature crack resistance of asphalt binders, this study conducted BBR tests on asphalt samples. Before the BBR testing, all asphalt samples underwent the PAV aging procedures. The aged asphalt samples were then tested using the BBR at temperatures of -12, -18, and -24°C, following the AASHTO T 313-2008 standard. The BBR test equipment used was the TE-BBR model BBR, made by Cannon, USA.

2.8 FTIR tests

Differences are noted in the intensities of functional groups within asphalt both before and after the aging process [25]. The FTIR test was performed to analyze the alterations in the functional groups of modified asphalt, based on the varying aging circumstances, and to gauge how different modified dosages affected asphalt's resistance to aging. The experiment was carried out using the Thermo Scientific Nicolet iS20 instrument, with a sweep range of 400-4,000 cm⁻¹, and was repeated 32 times.

2.9 Fluorescence microscopy tests

When subjected to ultraviolet radiation, various components within asphalt exhibit different levels of fluorescence intensity. Generally, the lighter components predominantly induce the fluorescence observed in asphalt, while asphaltene components contribute minimally to fluorescence. As the asphalt ages, the increased presence of asphaltene components and decreased concentration of lighter components leads to reduced fluorescence intensity. Consequently, assessing the average fluorescence intensity is a viable strategy to evaluate the anti-aging properties of asphalt [26]. For this experiment, the LEICADM4M fluorescence microscope from the German firm Leica was selected for fluorescence microscopy testing. Asphalt specimens were affixed to glass slides and examined under 400-fold magnification for detailed analysis of fluorescence intensity.

2.10 RTFOT mass loss rate, flash point, and ignition point tests

To assess the impact of modifiers on the stability and safety characteristics of asphalt binders, this study conducted tests to measure the RTFOT mass loss rate of both base and modified asphalts, along with flash and ignition point tests. The testing methodologies adhered to the guidelines specified in ASTM standards D2872 and D8254.

3 Results and discussion

3.1 High-temperature rheological properties

The results of temperature sweep for the complex shear modulus (G^*) are shown in Figure 3, where a higher G^* value indicated a higher hardness of the asphalt. The research findings suggested that adding modifiers overall

6 — Chuangmin Li et al. DE GRUYTER

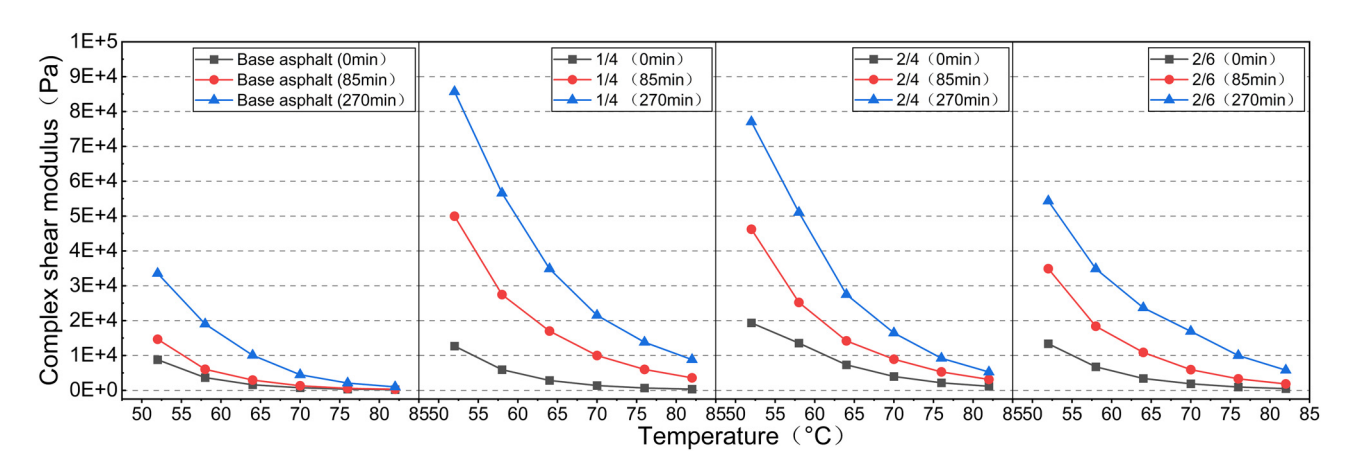


Figure 3: Complex shear modulus of asphalt binder with varying modifier contents and aging conditions.

increased the G^* values of the base asphalt under different aging conditions, effectively enhancing its resistance to deformation in various aging states. Additionally, for all asphalt binder types, the G^* values rose with aging time, indicating that aging leads to a greater degree of asphalt binder hardening.

For the unaged original composite asphalt, when the TPO dosage was fixed, G^* increased with the addition of PPA; inversely, when the PPA dosage was fixed, the G^* value of the asphalt binder decreased as the quantity of TPO rose. This suggests that while TPO lowers the high-temperature performance of the asphalt binder, the presence of PPA can effectively mitigate and improve the negative impacts of TPO on its high-temperature behavior.

In aged composite asphalt, a decrease in the G^* value was observed as the modifier dosage increased. This pattern demonstrates that the inclusion of modifiers can effectively reduce the phenomenon of the asphalt's hardening in the aging process. Among the three examined modified asphalts, the 2/6 asphalt binder exhibited the smallest variation in the G^* value under different aging time conditions. For instance, at 52°C, the overall standard deviation of the G^* value for the 2/6 asphalt binder across three different states (0, 85, 270 min) was 16736.5, which was reduced by 29 and 44% compared to the 1/4 and 2/4 modified asphalts, respectively (as shown in Table 4). This indicates that,

relative to PPA, an increase in TPO dosage has a more significant effect in reducing asphalt aging hardening, as TPO helps offset the loss of light components caused by thermal oxidative aging in the asphalt binder [27].

To quantitatively assess the impact of aging on the temperature sensitivity of asphalt binders quantitatively, the G^* values are used, employing Eq. (10) to fit the Complex modulus index (GTS) [28]. A smaller absolute value of GTS indicates lower temperature sensitivity for the asphalt binder. The fitting results for each parameter can be found in Table 5, while those specific to GTS values are shown in Figure 4.

$$\lg(\lg G^*) = GTS \lg(T) + C, \tag{10}$$

where G^* is the complex shear modulus in pascals, GTS represents the slope, T represents the test temperature in degree Celsius, and C represents the intercept.

The results in Figure 4 show that, except for the base asphalt, the |GTS| values of all other modified asphalts tend to decrease as aging time increases. However, the base asphalt under 85 min RTFOT aging conditions had exhibited a |GTS| value higher than the unaged base asphalt. This indicates that the base asphalt, once aged for 85 min RTFOT, reduced temperature sensitivity compared to when it is unaged. Similar observations have been made in the studies by Xue *et al.*, suggesting a connection to asphalt's unique

Table 4: Complex shear modulus and overall standard deviation of various asphalt binders at 52°C

Asphalt type and aging time	Base asphalt		1/4		2/4			2/6				
	0 min	85 min	270 min	0 min	85 min	270 min	0 min	85 min	270 min	0 min	85 min	270 min
Complex shear modulus Overall standard deviation	8773.3 10,572	14,646	33,551	12,696 29,802	49,969	85,689	19,359 23,569	46,228	77,045	13,360 16,737	34,901	54,338

Table 5: GTS fitting results for different types of asphalt binders

Asphalt type and aging time	GTS	С	R ²	Overall standard deviation
Base asphalt (0 min)	1.04266	2.36493	0.96600	0.1564
Base asphalt (85 min)	1.12750	2.55764	0.98261	
Base asphalt (270 min)	0.76153	1.94896	0.93353	
1/4 (0 min)	0.87970	2.10222	0.95216	0.1882
1/4 (85 min)	0.59716	1.69722	0.98944	
1/4 (270 min)	0.42291	1.41109	0.96672	
2/4 (0 min)	0.64686	1.73387	0.94203	0.0296
2/4 (85 min)	0.61812	1.72983	0.98774	
2/4 (270 min)	0.57492	1.67664	0.97055	
2/6 (0 min)	0.73816	1.86182	0.93787	0.1407
2/6 (85 min)	0.71420	1.88487	0.98607	
2/6 (270 min)	0.42837	1.40222	0.93512	

properties, particularly the ratios of components in the asphalt binder [29].

When discussing the impact of modifiers on the temperature sensitivity of asphalt binders, research findings showed that for the unaged original composite asphalt, the addition of modifiers could lessen the temperature sensitivity of the base asphalt. As modifiers were incorporated, the |GTS| value decreased with an increase in PPA content, while conversely, this value increased as the content of TPO rose.

Concerning the temperature sensitivity of aged composite asphalt, the |GTS| values of the 2/4 asphalt binder exhibited the least dispersion in three different states (0, 85, 270 min), showing an overall standard deviation of only 0.0296 (Table 5). This value is significantly lower than that

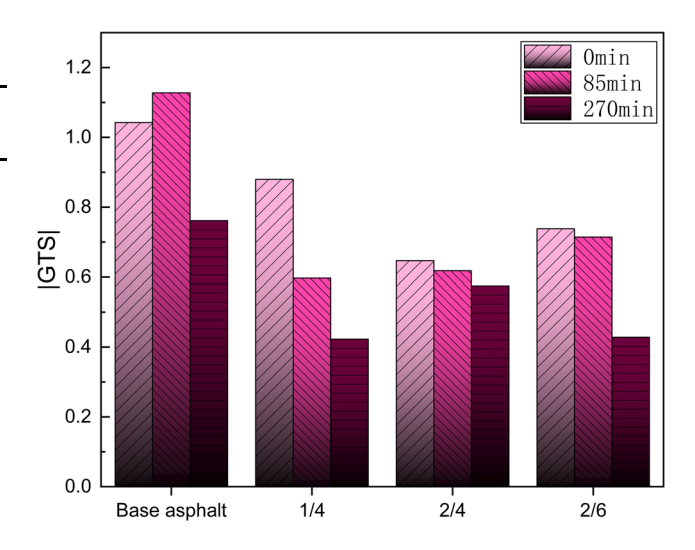


Figure 4: Absolute values of GTS for various types of asphalt binders.

of other modified asphalts, indicating that PPA improves the temperature sensitivity of asphalt binders and mitigates the impact of aging.

Figure 5 displays the temperature-sweep phase angle (δ), where smaller δ values indicate better elastic properties of the asphalt binder. In all asphalt binders, a decrease in δ values is observed as aging time increases, indicating enhanced resistance to deformation with aging. Furthermore, adding modifiers reduces the δ values in the base asphalt as it ages, suggesting that modifiers improve the base asphalt's elastic performance.

Regarding the unaged original composite asphalt, at a constant PPA content, an increase in TPO content led to a rise in the δ value of the asphalt binder. Conversely, at a fixed TPO content, the δ value of the asphalt binder decreased with an increase in PPA content. This phenomenon can be attributed to the oiliness of TPO, which softens the asphalt binder,

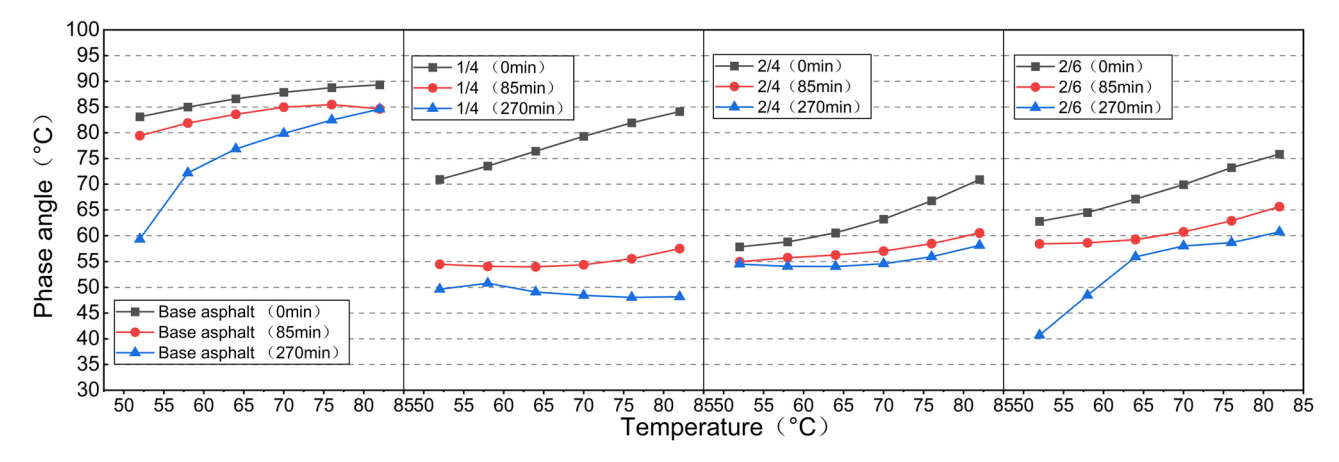


Figure 5: Phase angles of various types of asphalt binders.

while PPA interacts with the asphalt binder, transforming it from a sol-like state to a gel-like state [17].

In the case of aged composite asphalt, the fluctuation range of δ values for the 1/4 modified asphalt was broader under various temperature conditions. However, with the increased PPA content, as demonstrated by the 2/4 and 2/6 modified asphalt, the fluctuation range of δ values in these two asphalt binders was reduced compared to that of the 1/4 modified asphalt. This suggested that a higher PPA content led to a significant decrease in the fluctuation range of δ values in modified asphalt across various aging conditions. The reason for this is that more cross-linked macromolecular structures generate within the asphalt binder by increased PPA content, thereby ensuring a stable viscouselastic component under various aging scenarios [30].

To analyze how modifiers and aging influence the viscoelastic properties of asphalt binders, a black diagram is utilized. This diagram maps the phase angle data from the asphalt binder's temperature sweep onto the x-axis (abscissa) and the complex shear modulus on the y-axis (ordinate), as shown in Figure 6. The results indicated that for unaged original composite asphalt, the phase angle-complex shear modulus curve of the modified asphalt shifted to the left compared to the base asphalt, in the order: 1/4 < 2/6 < 2/4. This suggested that adding PPA improves the viscoelastic behavior of asphalt binders, while incorporating TPO is counterproductive. For aged composite asphalt, the curve shifted leftward with increased aging, indicating that aging enhances the asphalt binder's viscoelastic behavior.

Figure 7 displays the results for the rutting factor $(G^*/\sin \delta)$ of the asphalt binder across different aging

conditions. An increase in the rutting factor indicates enhanced stiffness and reduced plasticity of the asphalt binder. In this study, the addition of modifiers allowed for a varying degree of improvement in the base asphalt's rutting factor, indicating that the modifier positively contributes to bolstering the asphalt binder's stiffness. Furthermore, as the aging time increased, the rutting factor of the asphalt binder showed a growing trend, indicating that the aging process diminishes the asphalt binder's plasticity.

Regarding the unaged original composite asphalt, an escalation in PPA content served to increase its rutting factor, while an increment in TPO content triggered a reduction in this factor. This phenomenon is attributable to the fact that PPA reacts with asphalt, thereby increasing the asphaltene content within the binder [31]. However, the presence of numerous light components in TPO negatively influences its resistance to deformation.

In aged composite asphalt, an increasing TPO content reduced the rutting factor of modified asphalt. The No. 2/6 asphalt binder exhibited the smallest fluctuation in the rutting factor among the three types of modified asphalt under various aging time conditions. As an example, at 52° C, the overall standard deviation of the G^{*} values for the No. 2/6 asphalt binder at three different states (0, 85, 270 min) was 28145.79, the lowest value compared to the other three types of modified asphalt in Table 6. This indicates that increasing the TPO content mitigates the aging-induced effects on the asphalt binder's plasticity.

To thoroughly assess the influence of modifiers on asphalt's high-temperature rheological properties, the study employs the critical temperature as the evaluation metric. A

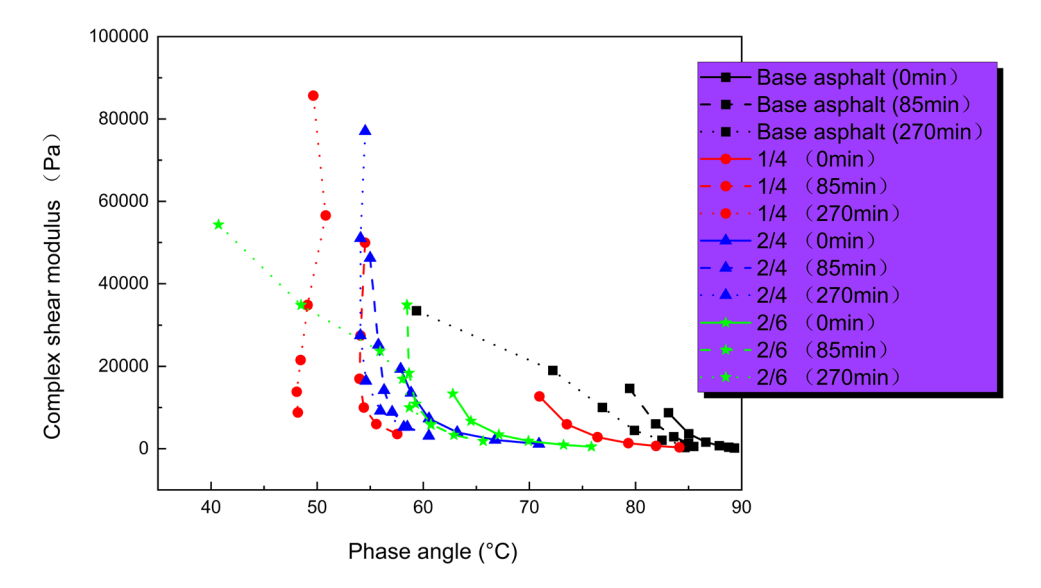


Figure 6: Black diagram of various types of asphalt binders.

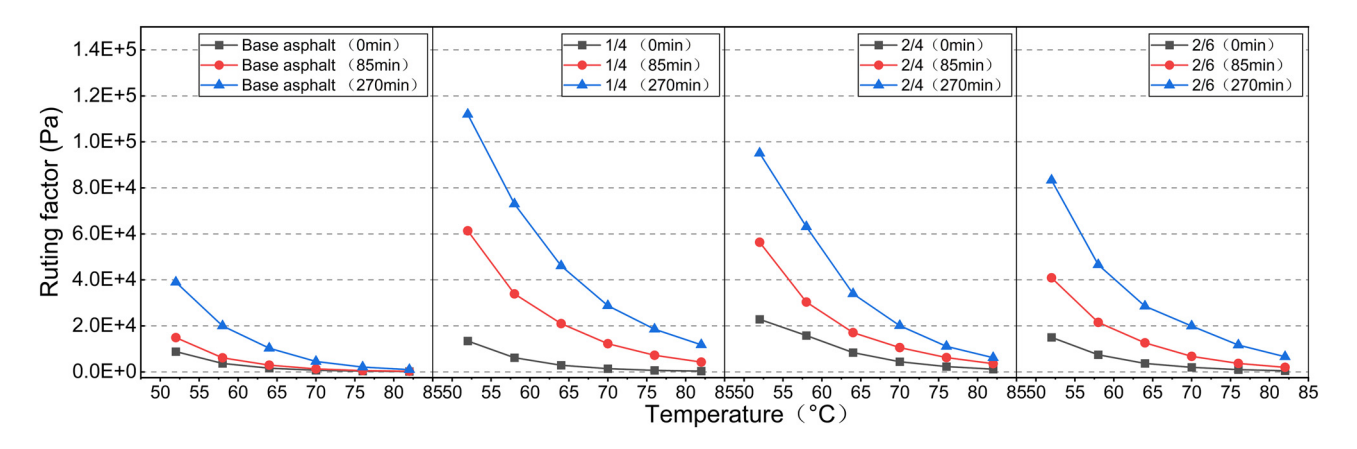


Figure 7: Rutting factor of various types of asphalt binders.

Table 6: Rutting factors of various types of asphalt binders at 52°C and overall standard deviation

Asphalt type and aging time	Base asphalt		1/4		2/4			2/6				
	0 min	85 min	270 min	0 min	85 min	270 min	0 min	85 min	270 min	0 min	85 min	270 min
Rutting factors Overall standard deviation	8837.3 13027.4	14,898 37	39,000	13,433 40244.8	, ,	11,2000	22,861 29516.5	,	95,100	15,024 28145.7	.,.	83,310

higher critical temperature indicates a higher maximum operating temperature limit. The critical high temperature ($T_{\rm C}({\rm High})$) for unaged asphalt binder is determined by Eqs. (11) and (12) and is applied to determine the critical high temperature ($T_{\rm C}({\rm High})$) for asphalt binder subjected to 85 min of RTFOT aging. The lesser of these two values denotes the critical high temperature [32].

$$T_{\rm C}({\rm High}) = \left(\frac{{\rm Log}(1.00) - {\rm Log}(G_1)}{a}\right) + T_1,$$
 (11)

$$T_{\rm C}({\rm High}) = \left(\frac{{\rm Log}(1.00) - {\rm Log}(G_1)}{a}\right) + T_1,$$
 (12)

where T_1 denotes a specific temperature in °C, G_1 represents the rutting factor ($G^*/\sin \delta$) at a specified temperature (T_1)

in kPa, and "a" represents the gradient of the stiffness-temperature curve.

Table 7 delineates the critical high temperatures for different asphalt binders. Overall, the integration of modifiers enabled a varying degree of enhancement in the base asphalt's high-temperature performance. For the three types of modified asphalt, the critical high temperature rose by 9.5, 33.5, and 14.7%, respectively, compared to the base asphalt. Furthermore, the asphalt binder's critical temperature ascended with an increase in PPA content and descended with a rise in TPO content. A comparison between the No. 1/4 and No. 2/4 asphalt binders reveals that a 1% increment in PPA content elevated the critical temperature of the No. 1/4 asphalt binder by 21.9%, indicating

Table 7: Critical high temperature of various types of asphalt binders

Asphalt type	Property	T_C (High) (°C)	Critical high temperature (°C)
Base asphalt	$G^*/\sin\delta$ (0 min)	67.19	66.25
	$G^*/\sin \delta$ (85 min)	66.25	
1/4	$G^*/\sin \delta$ (0 min)	72.51	72.51
	$G^*/\sin \delta$ (85 min)	88.36	
2/4	$G^*/\sin \delta$ (0 min)	83.45	83.45
	$G^*/\sin \delta$ (85 min)	87.46	
2/6	$G^*/\sin \delta$ (0 min)	75.90	75.90
	$G^*/\sin \delta$ (85 min)	81.27	

that PPA effectively suppresses and ameliorates the deleterious effects of TPO on the high-temperature performance of the asphalt binder. This phenomenon is attributed to the fact that PPA augments the quantity of heavy fraction within the asphalt binder [33].

3.2 LAS test results

Figure 8 presents stress—strain curves of asphalt binder subjected to varying aging periods. In these curves, there is an inverse relationship between the peak width of the asphalt binder and its stress dependency, and the peak width shows a positive correlation with the macromolecule content [34,35]. For both the unaged original composite asphalt and the aged composite asphalts, with constant TPO content, the peak width increased as the PPA content rose. Conversely, at a fixed PPA content, increasing the TPO content led to a narrower peak width in the asphalt binder. These findings indicate that the presence of PPA diminishes the asphalt binder's stress dependency while enhancing the macromolecule content. In contrast, TPO increases stress dependence and raises the small molecule content.

A nonlinear fitting of the LAS data, in accordance with AASHTO T 391-20, is performed for an in-depth analysis of the asphalt binder damage properties before and after aging. These data are subsequently normalized. The integrity parameter D(t) serves as the y-axis, and the cumulative damage parameter C(t) as the x-axis, for plotting the VECD damage curve of the asphalt binder (Figure 9). With a fixed C(t) value, a larger D(t) value indicates enhanced resistance

to damage under specific load conditions. An undamaged asphalt binder is indicated by a C(t) value of 1, which decreases to 0 when the asphalt binder is completely damaged.

Experimental outcomes demonstrated that within a limited damage range, all asphalt binder damage curves exhibited significant similarity. However, this was not the case in a wider damage range. For the unaged original composite asphalt, the damage resistance of the base asphalt was significantly better than that of other unaged modified asphalts. For the 85-min-aged composite asphalt, the 1/4 binder showed optimal damage resistance. Meanwhile, the 2/4 modified binder presented the best damage resistance in the context of the 270-min-aged composite asphalt. Nevertheless, the aforementioned discussion serves as an initial assessment of the load damage attributes of the asphalt binder. For a comprehensive evaluation of the fatigue life of the modified asphalt binder, it is imperative to base the evaluation on the damage criterion [34].

As shown in Figure 10, we calculated the fatigue life $(N_{\rm f})$ of the asphalt binder under various strain levels based on the damage criterion of VECD shear stress. A larger $N_{\rm f}$ value indicates a longer fatigue life of the asphalt binder. Experimental results showed that at a lower strain level, with the increase in aging time, the $N_{\rm f}$ value of the asphalt binder increased. However, when the strain exceeded a certain threshold, the $N_{\rm f}$ value of the asphalt binder decreased with the increase in aging time, which is consistent with the research results of other researchers [36]. For this study, we found that under lower strain conditions (Figure 10a), the addition of the modifier enhanced the fatigue life of the base asphalt under various aging

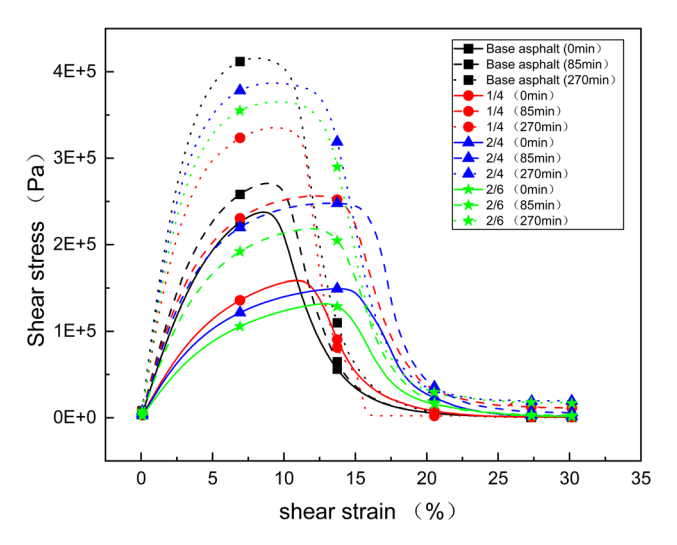


Figure 8: Stress–strain results of various types of asphalt binders under LAS test conditions.

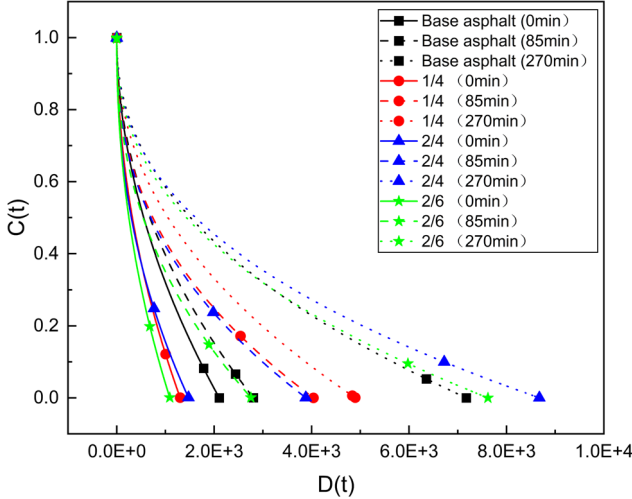


Figure 9: Stress–strain curves of various types of asphalt binders under LAS testing conditions.

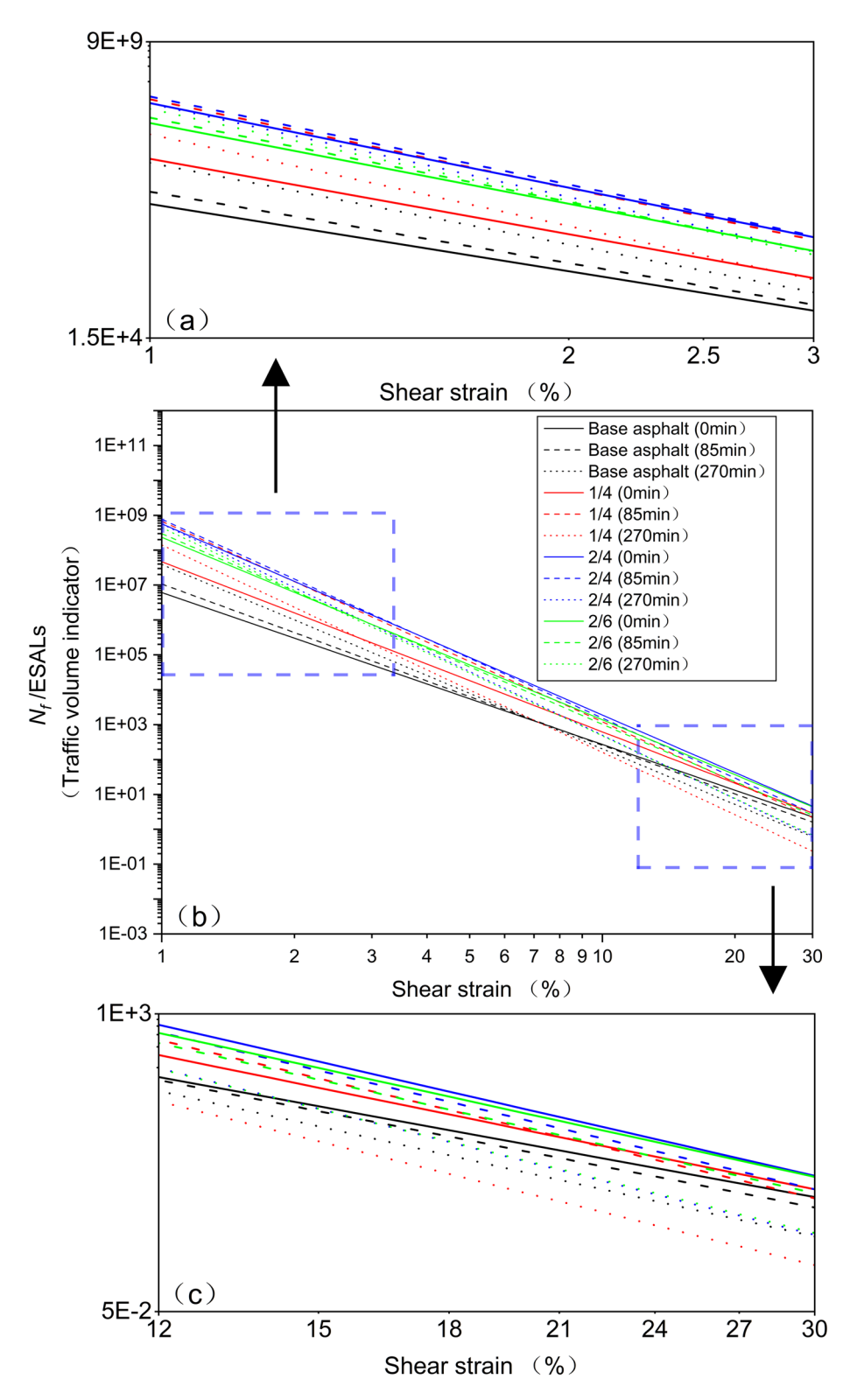


Figure 10: Fatigue life of various types of asphalt binders. (a) Low strain level condition, (b) Overall view, and (c) High strain level condition.

conditions. Whether in the unaged original composite asphalt or the aged composite asphalt, the 2/4 asphalt binder exhibited the longest fatigue life. By comparing

the 1/4 and 2/4 asphalt binders, we observed that an increase in PPA content significantly enhanced the fatigue resistance as indicated by $N_{\rm f}$ values of the asphalt binder

under different aging conditions. Furthermore, a comparison between the 2/4 and 2/6 asphalt binders revealed that although a rise in TPO content might have shortened the fatigue life of the asphalt binder under unaged or short aging (85 min) conditions, it decreased the range of variation in $N_{\rm f}$ values. This demonstrates that TPO, despite its potential to reduce the fatigue life under certain conditions, can mitigate the impact of aging on the fatigue resistance of the asphalt binder.

However, observing Figure 10c, when the asphalt binder was in a high strain level state, it was observed that both the unaged original composite asphalt and the aged composite asphalt demonstrated the pattern of their fatigue life rising and falling, respectively, with the increase in PPA and TPO content. Interestingly, the 270 min aged composite asphalt of sample 1/4 exhibited the lowest fatigue life ($N_{\rm f}$) value. However, with an upsurge in PPA content, the asphalt binder from sample 2/4 exceeded the $N_{\rm f}$ value of sample 1/4. This can be attributed to a possible threshold effect of PPA content on the

fatigue performance of long-term aged asphalt binder under significant strain. Only when the PPA content exceeds this threshold does it effectively enhance the fatigue performance of the long-term aged asphalt binder under high strain.

3.3 MSCR test results

As depicted in Figures 11–13, various types of asphalt binders exhibited varied strain response curves during the initial load cycle under distinct temperature and stress conditions. As anticipated, the maximum strain of the asphalt binder decreased with the progression of aging time and increased as the load level escalated. This outcome suggests that aging leads to a hardening of the asphalt binder, thereby reducing its deformation under load conditions. Moreover, with an increase in the test temperature, all asphalt binders demonstrate a trend of

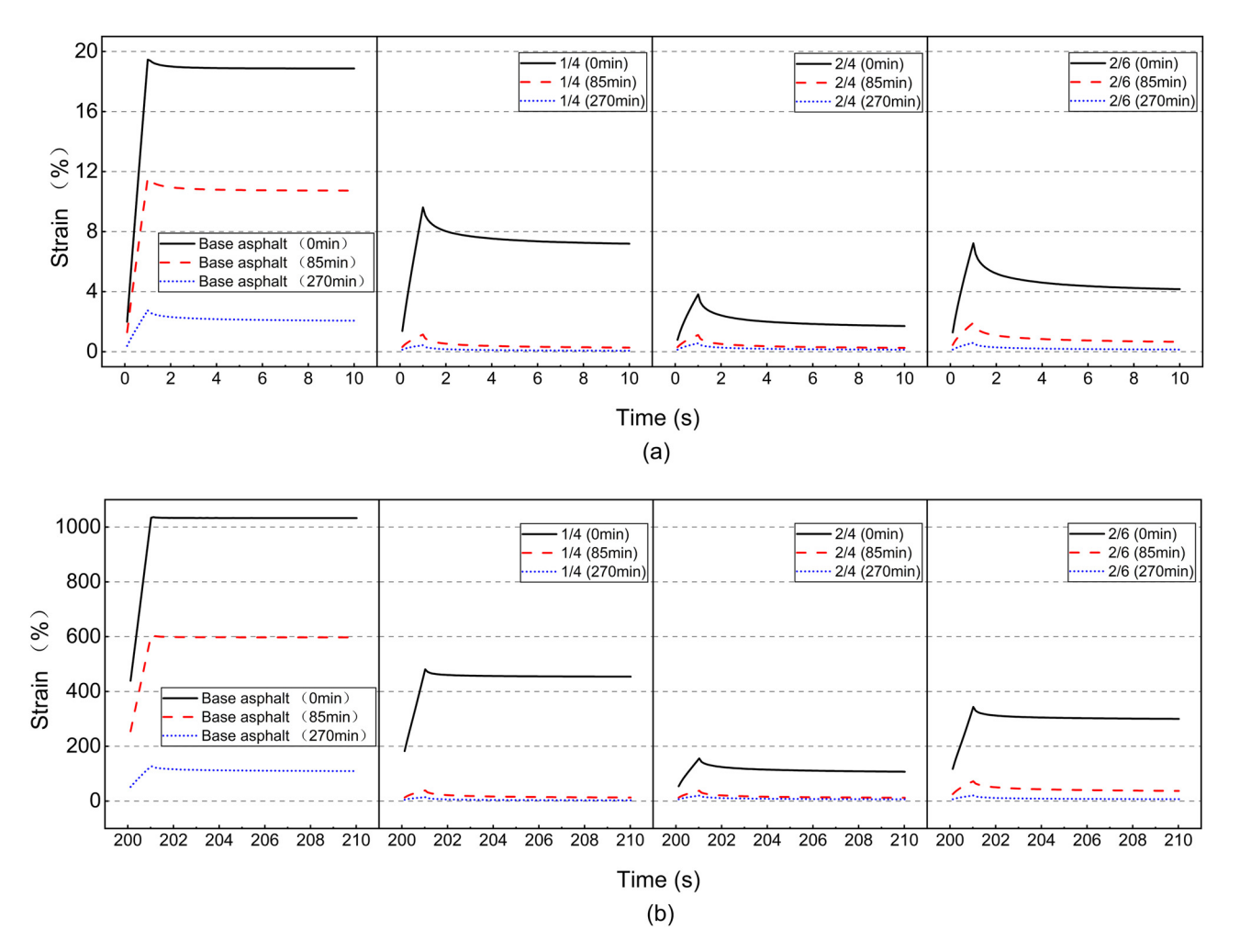


Figure 11: Strain response curves of various types of asphalt binders at 58°C: (a) 0.1 kPa and (b) 3.2 kPa.

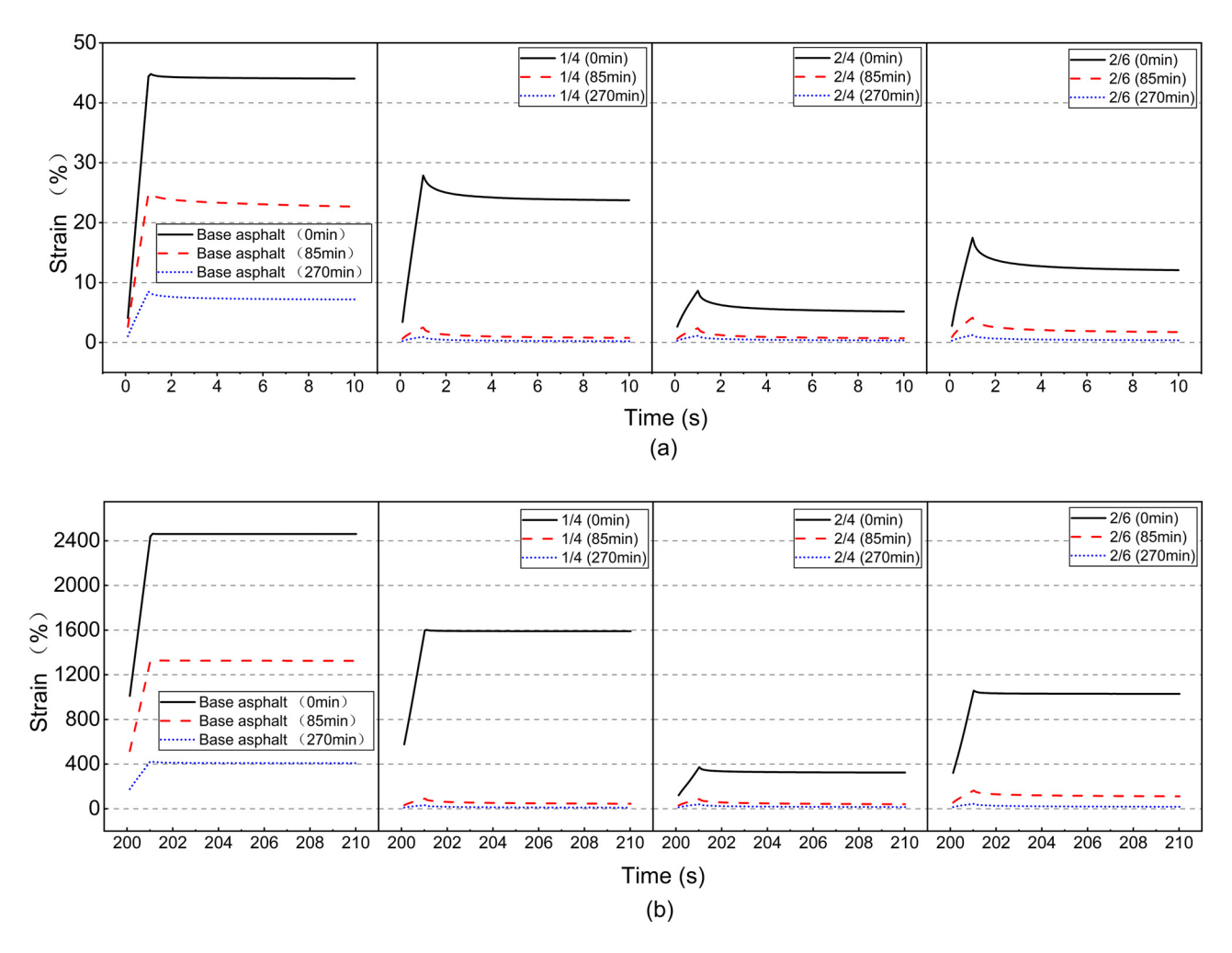


Figure 12: Strain response curves of various types of asphalt binders at 64°C: (a) 0.1 kPa and (b) 3.2 kPa.

greater strain amplitude with temperature elevation, indicating that higher temperatures adversely affect the asphalt binder's ability to resist deformation.

Under three distinctive temperature conditions, both unaged original composite asphalt and the aged composite asphalt consistently exhibited lower maximum strain values compared to the base asphalt under similar conditions. This observation suggests that the addition of modifiers substantially enhances the deformation resistance of the base asphalt. Using the strain response curves of various asphalt binders at 64°C and 0.1 kPa (Figure 12) for reference, when the TPO content was kept constant, increasing the PPA content lowered the maximum strain of the asphalt binder. Conversely, if the PPA content remained stable, an increase in TPO content resulted in increased maximum strain. This demonstrates that adding PPA effectively enhances the asphalt binder's deformation resistance and counteracts the effects of TPO.

For aged composite asphalt, the strain response curves of various types of asphalt binders at 64°C and 0.1 kPa, as

shown in Figure 12, were used as an example. When comparing asphalt binders No. 1/4 and No. 2/4, increasing the PPA content could mitigate the effects of aging on the asphalt binder, reduce the fluctuation of maximum strain under varying aging conditions, and promote stability. Conversely, a higher TPO content intensified aging's effects on the binder, increasing strain fluctuation, leading to instability. This is due to PPA's capacity to consume and convert light components to heavy ones in the asphalt binder, thereby lowering the percentage of oxidizable and loss-prone light components, thus preserving binder stability during aging. TPO helps replenish light components lost to thermal oxidation, consequently extending the complete aging timeline for the binder.

Figures 14 and 15 display the evaluation indicators of the MSCR tests performed at three different temperatures. $R_{0.1}$ and $R_{3.2}$ represent the recovery percentages of the asphalt binder under test conditions of 0.1 and 3.2 kPa, and R-diff represents the difference in recovery

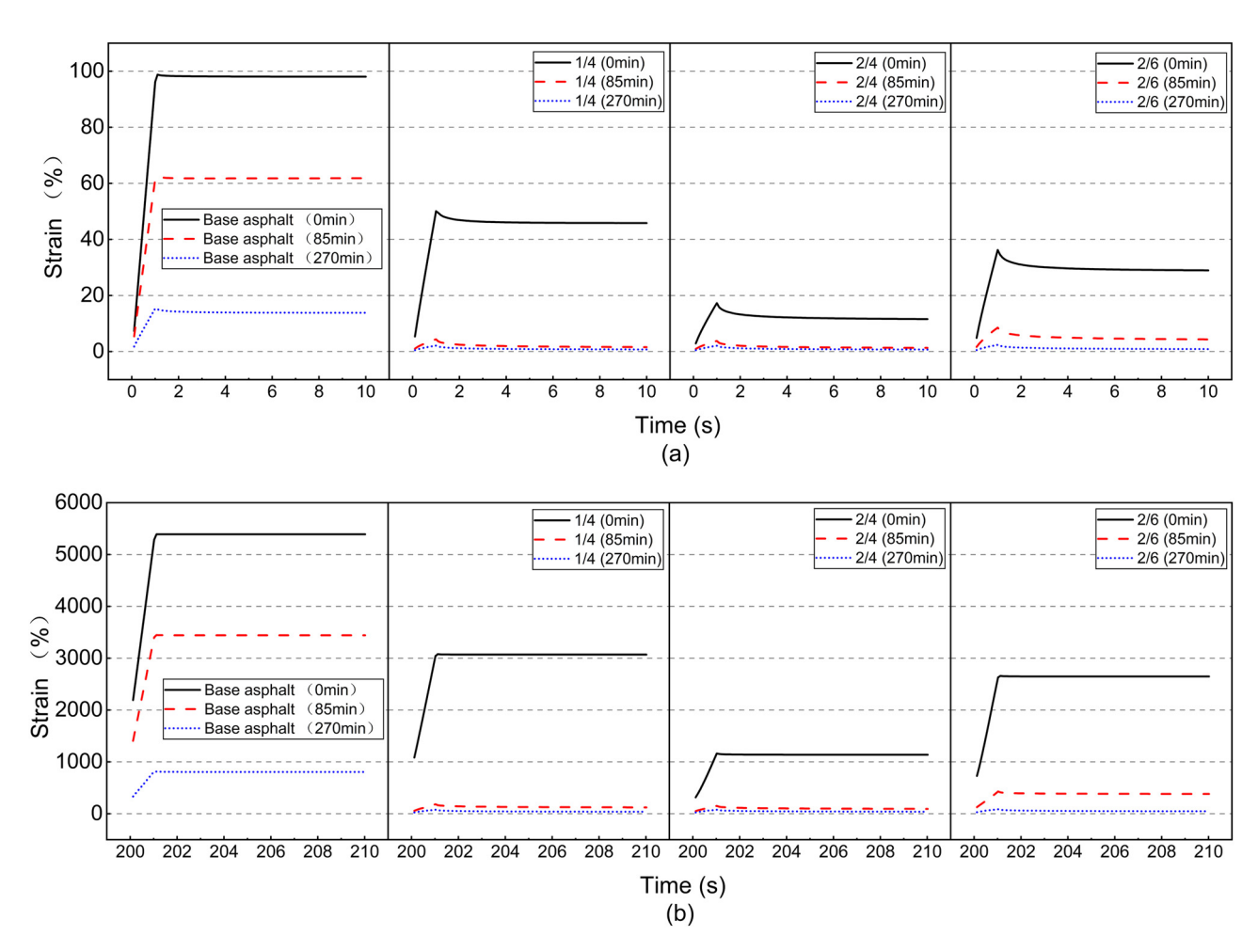


Figure 13: Strain response curves of various types of asphalt binders at 70°C: (a) 0.1 kPa and (b) 3.2 kPa.

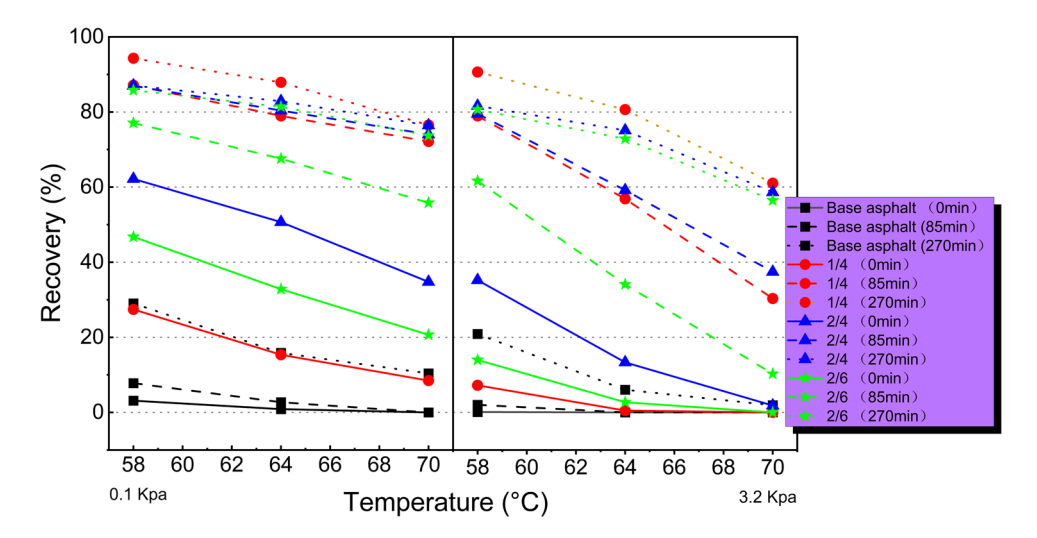


Figure 14: Percent recovery of various types of asphalt binders.

percentages of the asphalt binder under test conditions of 0.1 and 3.2 kPa. In general, a larger R value indicates greater elasticity in the asphalt binder, and a smaller R-diff value suggests a slight impact of stress on its elastic recovery ability.

The R value of the asphalt binder increased with prolonged aging and decreased as the load increased. This indicated that aging reduces the total strain of the asphalt binder under a fixed load, thereby increasing the creep recovery rate; that is, under a lower load level, the asphalt binder is more likely to exhibit elastic behavior. For our research, the R values of base asphalt and modified asphalt showed a linear relationship in the range of $58-70^{\circ}$ C; that is, as the temperature rose, the R values decreased.

For unaged original composite asphalt and aged composite asphalt for 85 min, by comparing asphalt binders No. 1/4 and No. 2/4, we found that an increase in PPA content could increase and decrease the *R* values and R-diff values of the asphalt binder under different temperature and load conditions. However, when the TPO content was further increased on the basis of No. 2/4 asphalt binder, the *R* values and R-diff values of No. 2/6 asphalt binder actually decreased and increased. This indicates that the addition of PPA can improve the rutting resistance of the asphalt binder, while it reduces the extent to which its elastic recovery is affected by stress, while the addition of TPO is harmful to the deformation recovery of the asphalt binder under load conditions.

However, for aged composite asphalt for 270 min, No. 1/4 asphalt binder had actually demonstrated the highest R values and the lowest R-diff values. When the modifier content was increased beyond No. 1/4 asphalt binder, the

R values of the asphalt binder decreased, and the *R*-diff values increased. This implies that under long-term aging conditions, the excessive addition of modifiers would negatively impact the asphalt binder's elastic properties.

Figures 16 and 17 display the results of the $J_{\rm nr}$ and $J_{\rm nr-diff}$ from the MSCR experiments on various asphalt binders. Generally, a higher $J_{\rm nr}$ value indicates a greater permanent deformation of the asphalt binder under load, while a larger $J_{\rm nr-diff}$ value suggests a greater disparity in permanent deformation across different load conditions. The results demonstrated that, for various asphalt binders, the $J_{\rm nr}$ values increased with the rising test temperatures and decreased with increased aging. This suggests that asphalt binders are more prone to permanent deformation at high-temperature load conditions, while aging mitigates the deformation caused by loading in these binders.

For unaged original composite asphalt, the addition of modifiers effectively reduced permanent deformation under various load conditions compared to base asphalt. Compared to the $J_{\rm nr}$ values of the 1/4 and 2/4 asphalt binders, the 2/4 binder consistently showed the lowest $J_{\rm nr}$ values under various stress conditions. This indicates that incorporating PPA into the asphalt binder reduces its permanent deformation under loading. However, increasing the TPO content in the asphalt binder, as demonstrated by the 2/6 binder, resulted in higher $J_{\rm nr}$ values. This suggests that adding TPO to the asphalt binder leads to an increase in its permanent deformation under load conditions.

In the case of aged composite asphalt, compared to other asphalt binders, the No. 2/4 asphalt binder shows less variability in $J_{\rm nr}$ value under different aging conditions. This indicates that an increase in PPA content can

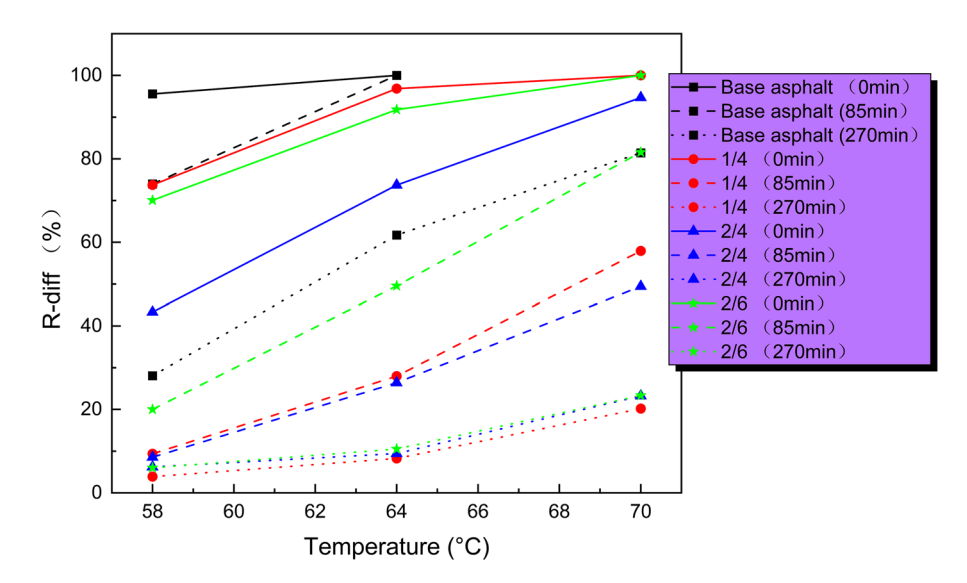


Figure 15: Percent recovery difference of various types of asphalt binders.

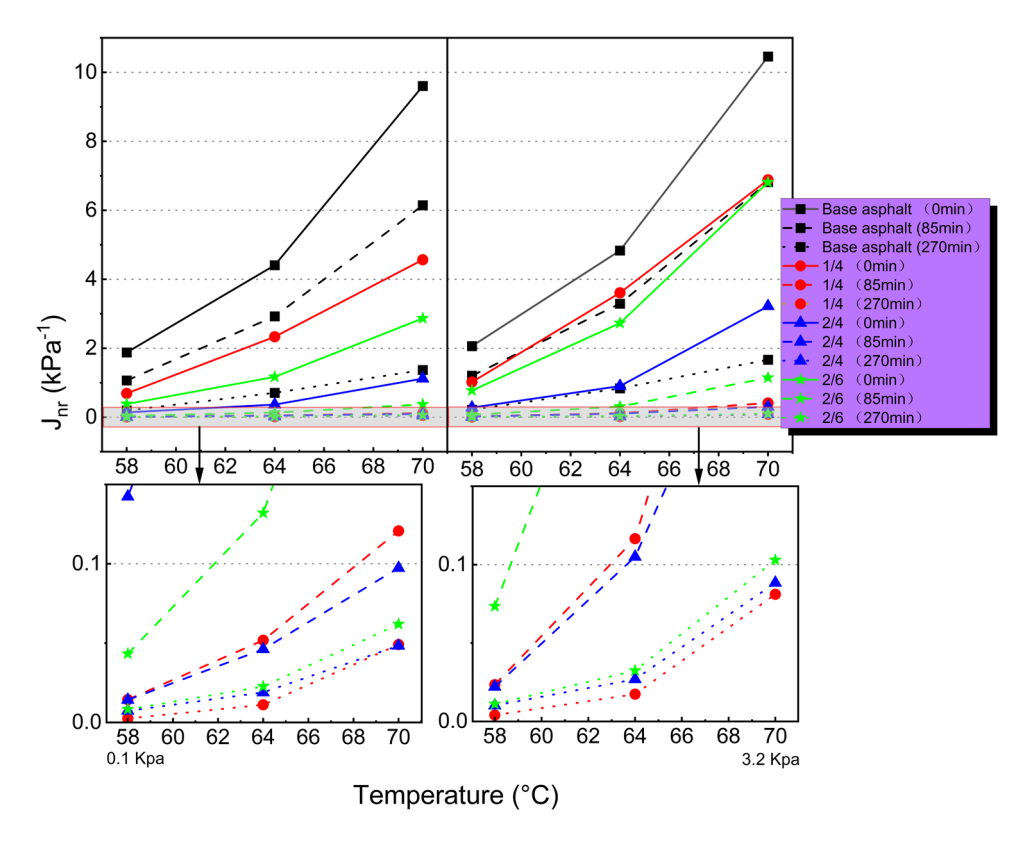


Figure 16: J_{nr} results of different asphalt binders.

reduce the variation in permanent deformation caused by aging in asphalt binders. However, $J_{\rm nr\text{-}diff}$ data indicated that although modifiers improve the base asphalt's resistance to permanent deformation, they also raise the asphalt binder's $J_{\rm nr\text{-}diff}$ value. This implies that adding modifiers can exacerbate the base asphalt's variability in permanent deformation under various load conditions.

3.4 BBR test results

Figures 18 and 19 illustrate the creep stiffness (S) and creep rate (m) of asphalt binders under a 60 s load at various temperatures. The results indicated that, with the decrease in the temperature, the S values increase while the m values decrease. This suggests that at lower temperatures,

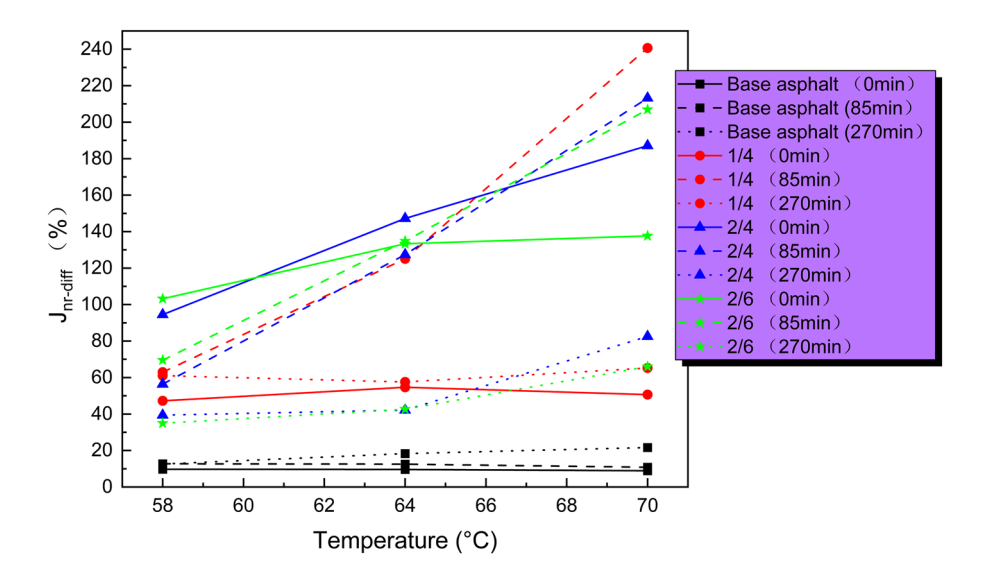


Figure 17: $J_{\text{nr-diff}}$ results of different asphalt binders.

DE GRUYTER

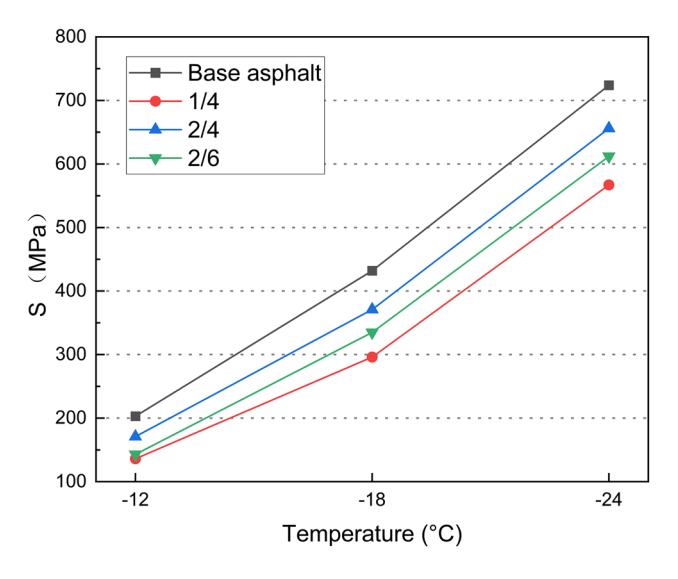


Figure 18: Creep stiffness of asphalt binders at different temperatures.

asphalt binders become more susceptible to cracking and damage.

In comparison to the base asphalt, all modified asphalts exhibited reduced *S* values and increased m values. This indicated an effective enhancement in the low-temperature crack resistance of asphalt binders due to the addition of modifiers. Furthermore, when comparing the S and m values between the 1/4 and 2/4 asphalt binders, it was observed that the 2/4 asphalt binder exhibited higher *S* values and lower m values. This suggests that the addition of PPA makes the asphalt binder more brittle at low temperatures, negatively impacting its low-temperature crack

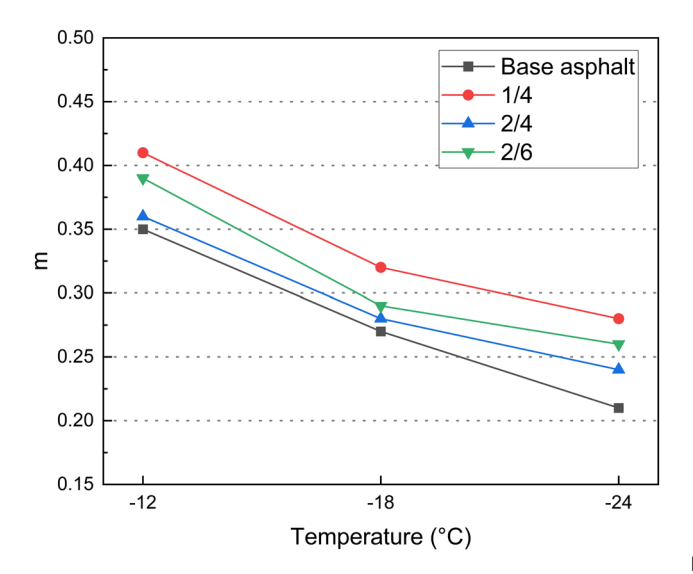
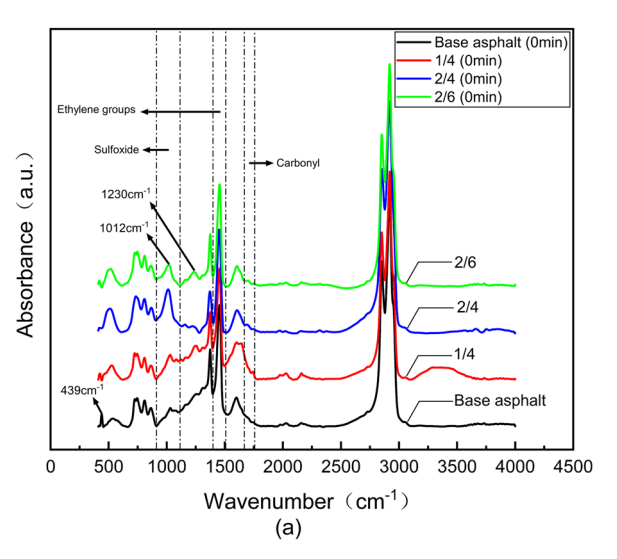
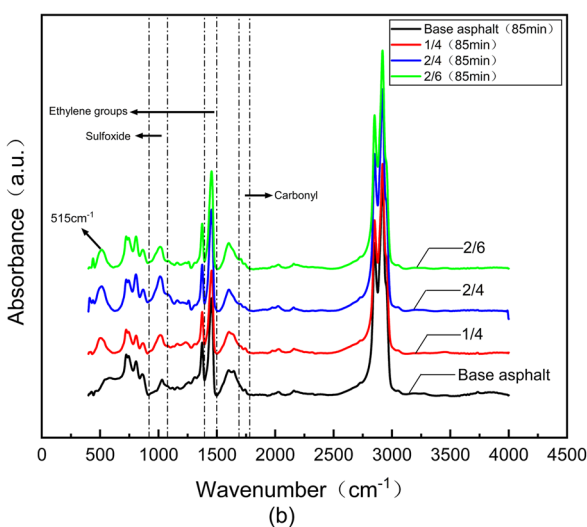


Figure 19: Creep rate of asphalt binders at different temperatures.





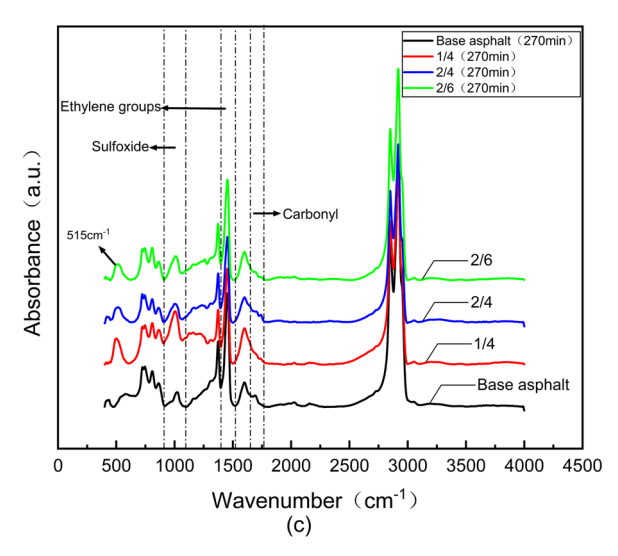


Figure 20: FTIR results of asphalt binder at different aging times: (a) 0 min, (b) 80 min, and (c) 270 min.

18 — Chuangmin Li et al. DE GRUYTER

Table 8: Position of the significant peaks of asphalt binder and their corresponding functional groups

Ref.	Peak position	Functional groups	Details
[38]	439	Si-O-Si	Bending vibration
[39]	515	Si-O-Al	Functional groups
[40]	733	-CH ₂	Rocking
[37]	1,012	P-O-C	Ester; stretching
[40]	1,373	CH ₃	Aliphatic; plan deformation
[40]	1,451	CH ₃ and CH ₂	Aliphatic; deformation
[40]	1,600	C = C	Conjugated ring vibration
[40]	2,850	C-H	Aliphatic hydrogen; CH ₂ ; symmetric stretching
[40]	2,919	С-Н	Aliphatic hydrogen; CH ₃ and CH ₂ ; Asymmetric stretching

resistance. However, a comparison between the 2/4 and 2/6 asphalt binders revealed that the 2/6 asphalt binder exhibited smaller *S* values and larger m values. This implies that increasing the TPO content in modified asphalt results in superior low-temperature crack resistance. This phenomenon is attributable to the softening effect of TPO on the asphalt, which enhances its ductility at lower temperatures.

3.5 FTIR spectroscopy test results

In an effort to delve into the physicochemical interactions of asphalt with its modifiers before and after aging, we perform FTIR tests. The smoothing and baseline correction of the results enable clearer observation of changes in functional groups induced by the application of modifiers. Figure 20 and Table 8, respectively, present the post-processing outcomes and the significant characteristic peaks and their affiliated functional groups.

The results showed that for the unaged original composite asphalt, after adding modifiers, the absorption peak at 439 cm⁻¹ vanished, which corresponded to the bending vibration of Si–O–Si. Concurrently, a notable increase was observed in the intensity of the absorption peak at 1,012 cm⁻¹. Comparing samples 1/4 and 2/4, a rise in PPA concentration leads to an increase in this peak intensity, attributable to the phosphatization of asphalt's –OH group [37]. Additionally, comparing samples 2/4 and 2/6 showed a decrease in the absorption peak around 1,230 cm⁻¹ (characteristic of PPA), aligning with an increase in the TPO content. This suggests a potential interaction between TPO and PPA, leading to PPA consumption. For the aged composite asphalt, a new absorption peak associated with the Si–O–Al functional group appeared

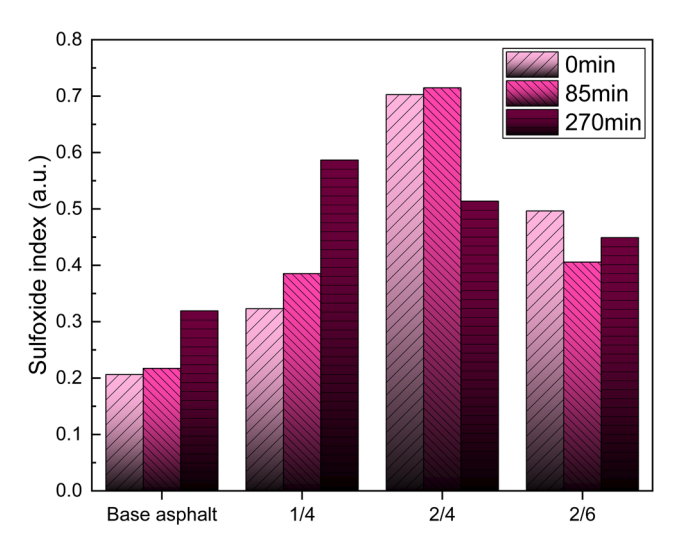


Figure 21: Sulfoxide index of various types of asphalt binders.

at 515 cm⁻¹, differing from the base asphalt. The disparity in these absorption peaks indicates physicochemical interactions between asphalt, its modifiers, and the PPA and TPO entities, regardless of the aging state.

Asphalt has undergone thermal oxidation during the aging process, leading to the oxidation of the asphalt and changes in the intensity of certain functional groups. Importantly, there has been significant increase in the intensity of sulfoxide (S=O) and carbonyl (C=O) groups during the aging process [40]. This has formed a crucial foundation for assessing the impact of aging on asphalt binders by analyzing functional group intensity changes before and after aging. In this study, semi-quantitative analysis, using the sulfoxide index (ratio of sulfoxide to ethylene group intensity) and carbonyl index (ratio of carbonyl to ethylene group intensity), has been employed to further investigate the impact of modifiers on asphalt aging. In

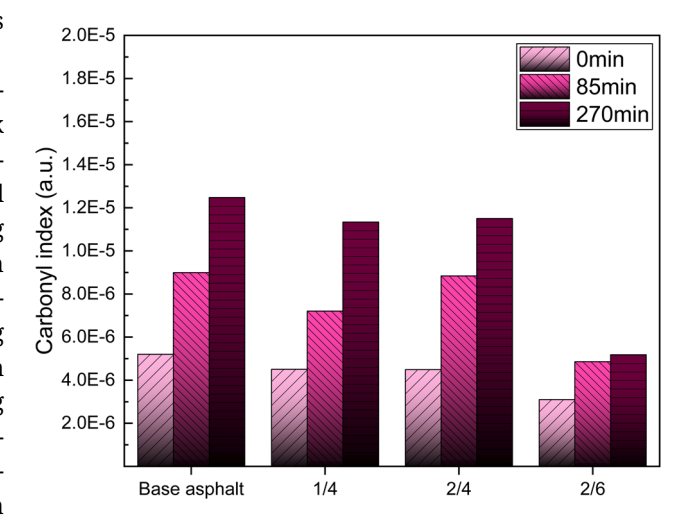


Figure 22: Carbonyl index of various types of asphalt binders.

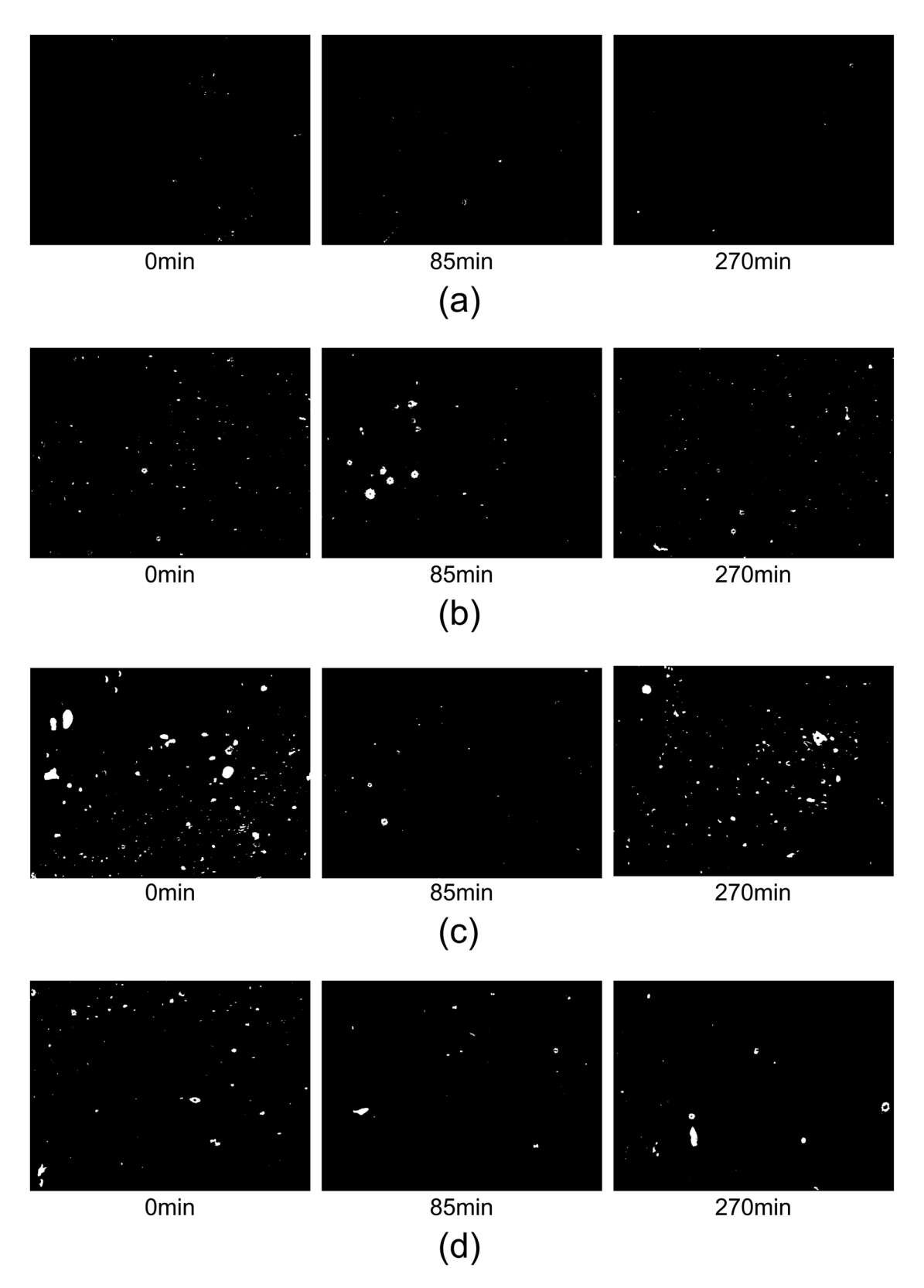


Figure 23: Fluorescence images of various types of asphalt binders after binarization: (a) Base asphalt, (b) 1/4, (c) 2/4, and (d) 2/6.

20 — Chuangmin Li et al. DE GRUYTER

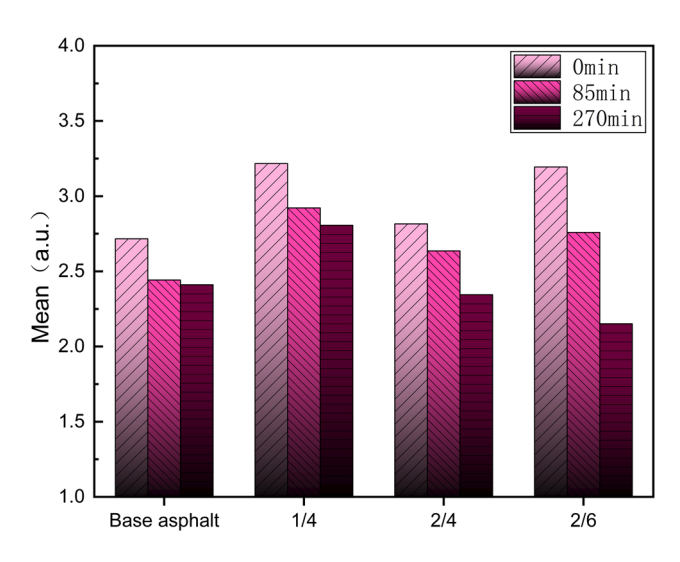


Figure 24: Average fluorescence intensity of various types of asphalt binders.

this context, the ethylene group (CH₂) has been deemed a functional group that is less affected by aging [41]. To guarantee the authenticity of the results, intensity data for the sulfoxide, carbonyl, and ethylene groups rely solely on unaltered raw FTIR data, with no smoothing or baseline correction. Finally, the processing results of the sulfoxide index and carbonyl index are shown in Figures 21 and 22.

The results show that adding a modifier to the base asphalt, either before or after aging, increased its sulfoxide index with noticeable variability. This phenomenon is attributed to the variety of sulfur-containing compounds in TPO, including thiophene, benzothiazole, and benzothiophene [42]. This indicates that for modified asphalt containing TPO, the sulfoxide index is not a reliable indicator of its aging level. In this study, however, the carbonyl index displayed a more consistent trend, with all asphalt binders showing an increase in this index as aging progressed. Discussing the impact of modifiers on asphalt's anti-aging properties, the modified samples 2/6 had the lowest carbonyl index and the least variation compared to other binders. The modified samples 1/4 and 2/4 showed a similar carbonyl index. This suggests that the addition of TPO can effectively mitigate the impact of thermo-oxidative aging on asphalt binders, whereas PPA does not have a significant effect on the resistance to thermo-oxidative aging on asphalt binders. This is due to TPO's relatively lower polarity compared to asphalt. Thus, during extended thermo-oxidative aging, TPO is preferentially oxidized, consuming thermal energy and oxygen. This indirectly lessens thermo-oxidation's impact on the asphalt binder itself.

3.6 Fluorescence microscopy test results

To investigate the microscopic morphology of modifiers in asphalt and assess the fluorescence intensity of asphalt binders, we use ImageJ software for processing the original images captured from fluorescence microscopy. To ensure comparability of results while optimally selecting signals from the modifier and minimizing those from the asphalt background, the threshold range of the algorithm is set between 13 and 255. In this study, the mean fluorescence intensity is calculated using Eq. (13). A reduced mean fluorescence intensity indicates a severe aging effect on the asphalt binder and significant loss of lighter components. The post-threshold processing results, along with the mean fluorescence intensity before and after aging of different modifier proportions, are presented in Figures 23 and 24.

$$Mean = \frac{IntDen}{Area},$$
 (13)

where Mean represents the mean fluorescence intensity of the region; IntDen is the total fluorescence intensity; and Area is the area of the region.

In the results of binarization, the asphalt phase is represented by the black region, while the prominently visible white region symbolizes the modifier phase. Calculations of mean fluorescence intensity showed a consistent decrease in the overall mean fluorescence intensity of various types of asphalt during aging, indicating an increase in the asphaltene content in the asphalt with prolonged aging. Regardless of the aging conditions, the modified asphalt with a PPA and TPO ratio of 1/4 exhibited the highest mean fluorescence intensity compared to other modified asphalts. Whether the unaged original composite asphalt or the aged composite asphalt that underwent 85 min of aging treatment, the trend

Table 9: Different asphalt binder mass loss rates, flash point, and fire point results

Property	Unit	Base asphalt	1/4	2/4	2/6
Flash point (ASTM D 92 standard)	°C	254	241	245	237
Fire point (ASTM D 92 standard)	°C	260	245	251	240
RTFOT mass variation (ASTM D2872 standard)	%	+0.5	+0.316	+0.337	0.013

in mean fluorescence intensities remained consistent (1/4 > 2/6 > 2/4 > Base asphalt). When PPA content is constant and TPO content is increased, the mean fluorescence intensity rose with the increase in TPO content, suggesting that addition of TPO can decrease the overall asphaltene proportion in the asphalt, mitigating the effects of short-term aging. Conversely, when the TPO content is constant and the PPA content is increased, the mean fluorescence intensity decreased with the rise in PPA, indicating that PPA can interact with asphalt to produce more asphaltene, consistent with previous study results [43].

Nevertheless, for aged composite asphalt subjected to a 270 min aging treatment, the mean fluorescence intensity trend of the asphalt binder altered, with its ranking by mean fluorescence intensity being 1/4 > Base asphalt > 2/4 > 2/6. It was noteworthy that, while maintaining a constant content of PPA, a decrease in the mean fluorescence intensity of the asphalt binder was observed with the increase in the content of TPO. This phenomenon can be explained by the following mechanism: the primary component of TPO is a light fraction. When an excessive amount of TPO is added to the asphalt binder, the surplus light fractions brought by TPO cannot be fully absorbed by the asphaltenes. This leads to the unabsorbed light fractions remaining in a free state, thereby increasing their exposure to oxygen and consequently promoting oxidation. Such oxidation results in the formation of more asphaltenes, which in turn reduces the mean fluorescence intensity of the asphalt binder.

3.7 Stability and safety

As Table 9 demonstrates, adding modifiers to base asphalt lowered its flash and fire points. A comparison of the 2/4 and 2/6 modified asphalts showed that increasing TPO content in the asphalt binder decreased its flash and fire points. In contrast, higher PPA content in the binder increased its flash and ignition points. Regarding the RTFOT mass variation, the data indicated that modifiers accelerated the base asphalt's mass loss rate, enhancing its volatility. An increase in TPO content was linked to a higher mass loss rate in the binder. However, a rise in PPA content in modified asphalt did not significantly alter the rate of mass variation, as the 1/4 and 2/4 modified asphalts demonstrated. These effects can be attributed to the volatile components in TPO, which make the binder more ignitable and increase the volatile fraction in modified asphalt. Conversely, PPA's ability to transform lighter asphalt components into larger molecules makes the binder more resistant to thermal oxidation.

4 Conclusion

This study conducts a series of experiments to explore the feasibility of using PPA/TPO as anti-aging modifiers for asphalt, leading to the following conclusions:

- 1) The presence of PPA in PPA/TPO modified asphalt has mitigated and enhanced the adverse effects of TPO on the high-temperature performance of the modified asphalt, while ensuring its low-temperature crack resistance. Additionally, while TPO presence has adversely affected the high-temperature performance of modified asphalt, it significantly slows the hardening effect caused by
- 2) In terms of the mechanical response of PPA/TPO modified asphalt, the addition of PPA has improved its fatigue resistance under aging conditions and lessened the impact of aging on its deformation resistance.
- Regarding the thermo-oxidative aging resistance of PPA/ TPO modified asphalt under thermal and oxygen conditions, TPO, due to its higher polarity, can be preferentially oxidized by oxygen, thus reducing the impact of oxygen on the asphalt binder itself.
- For modified asphalt containing TPO, due to the presence of a substantial number of sulfur-containing substances in TPO, it is not recommended to use the sulfoxide index as a measure for the anti-aging behavior of TPO-modified asphalt, in comparison to the carboxyl index.
- 5) The results of the FTIR and fluorescence microscopy tests indicate that, regardless of whether in an unaged or aged state, there is a physicochemical interaction between the asphalt and the modifiers, PPA, and TPO. Furthermore, an increase in the PPA content within the modified asphalt is manifested by a reduction in the fluorescence intensity of the modified asphalt, suggesting that PPA reacts with the asphalt binder to produce more asphaltenes.

In summary, this research has confirmed the feasibility of PPA/TPO as anti-aging modifiers for asphalt. However, performance tests on TPO and PPA modified asphalt mixtures, including low-temperature performance tests, are yet to be conducted. Therefore, before deploying TPO and PPA modified asphalt in actual projects, it is critical to perform further tests assessing the road performance of these mixtures, including evaluations of water stability and freezethaw resistance.

Acknowledgments: This work was supported by the science and technology project of Jiangxi provincial department of transportation (2023H0025); Science and technology

project of Jiangxi provincial department of transportation (2020H0023); Postgraduate research innovation project of Changsha university of science and technology in 2023 (CSLGCX23022); The authors would like to thank Shiyanjia Lab (www.shiyanjia.com) for the FTIR tests.

Funding information: This work was supported by the science and technology project of Jiangxi provincial department of transportation (2023H0025); Science and technology project of Jiangxi provincial department of transportation (2020H0023); Postgraduate research innovation project of Changsha university of science and technology in 2023 (CSLGCX23022).

Author contributions: Chuangmin Li: project administration; Lubiao Liu: performing the experiment, data analysis, and writing; Youwei Gan: supervision; Qinhao Deng: language modification; and Shuaibing Yi: syntax check. All authors have accepted responsibility for the entire content of this manuscript and approved its submission.

Conflict of interest: The authors state no conflict of interest.

Data availability statement: The datasets generated during and/or analyzed during the current study are available from the corresponding author on reasonable request.

References

- [1] Hou, X., F. Xiao, J. Wang, and S. Amirkhanian. Identification of asphalt aging characterization by spectrophotometry technique. *Fuel*, Vol. 226, 2018, pp. 230–239.
- [2] Saleh, N. F., B. Keshavarzi, F. Yousefi Rad, D. Mocelin, M. Elwardany, C. Castorena, et al. Effects of aging on asphalt mixture and pavement performance. *Construction and Building Materials*, Vol. 258, 2020, id. 120309.
- [3] Zhang, Y., Z. Zhang, A. M. Wemyss, C. Wan, Y. Liu, P. Song, et al. Effective thermal-oxidative reclamation of waste tire rubbers for producing high-performance rubber composites. ACS Sustainable Chemistry & Engineering, Vol. 8, No. 24, 2020, pp. 9079–9087.
- [4] Machin, E. B., D. T. Pedroso, and J. A. de Carvalho. Energetic valorization of waste tires. *Renewable and Sustainable Energy Reviews*, Vol. 68, 2017, pp. 306–315.
- [5] Kumar, A., R. Choudhary, and A. Kumar. Aging characteristics of asphalt binders modified with waste tire and plastic pyrolytic chars. *PLoS One*, Vol. 16, No. 8, 2021, id. e0256030.
- [6] Sathiskumar, C. and S. Karthikeyan. Recycling of waste tires and its energy storage application of by-products – a review. Sustainable Materials and Technologies, Vol. 22, 2019, id. e00125.
- [7] Chen, A., Q. Deng, Y. Li, T. bai, Z. Chen, J. Li, et al. Harmless treatment and environmentally friendly application of waste tires –

- TPCB/TPO composite-modified bitumen. *Construction and Building Materials*, Vol. 325, 2022, id. 126785.
- [8] Tosun, H. B. Production and characterisation of waste tire pyrolytic oil – Investigating physical and rheological behaviour of pyrolytic oil modified asphalt binder. *Heliyon*, Vol. 9, No. 1, 2023, id. e12851.
- [9] Zhang, G., F. Chen, Y. Zhang, L. Zhao, J. Chen, L. Cao, et al. Properties and utilization of waste tire pyrolysis oil: A mini review. Fuel Processing Technology, Vol. 211, 2021, id. 106582.
- [10] Norambuena-Contreras, J., L. E. Arteaga-Pérez, J. L. Concha, and I. Gonzalez-Torre. Pyrolytic oil from waste tyres as a promising encapsulated rejuvenator for the extrinsic self-healing of bituminous materials. *Road Materials and Pavement Design*, Vol. 22, No. sup1, 2021, pp. S117–S133.
- [11] Kumar, A., R. Choudhary, and A. Kumar. Evaluation of waste tire pyrolytic oil as a rejuvenation agent for unmodified, polymermodified, and rubber-modified aged asphalt binders. *Journal of Materials in Civil Engineering*, Vol. 34, No. 10, 2022, id. 04022246.
- [12] Kumar, A., R. Choudhary, and A. Kumar. Characterization of storage stability of EPDM rubberized asphalt with tire pyrolytic oil and sulfur. *Journal of Materials in Civil Engineering*, Vol. 35, No. 5, 2023, id. 04023067.
- [13] Kumar, A., R. Choudhary, and A. Kumar. A study on aging characteristics of asphalt binders modified with waste EPDM rubber and tire pyrolysis oil. *Journal of Materials in Civil Engineering*, Vol. 35, No. 12, 2023, id. 04023473.
- [14] Kumar, A., R. Choudhary, and A. Kumar. Composite asphalt binder modification with waste non-tire automotive rubber and pyrolytic oil. *Materials Today: Proceedings*, Vol. 61, 2022, pp. 158–166.
- [15] Al-Sabaeei, A., M. Napiah, M. Sutanto, N. Z. Habib, N. Bala, I. Kumalasari, et al. Application of nano silica particles to improve high-temperature rheological performance of tyre pyrolysis oilmodified bitumen. *Road Materials and Pavement Design*, Vol. 23, No. 9, 2022, pp. 1999–2017.
- [16] Al-Sabaeei, A. M., M. B. Napiah, M. H. Sutanto, W. S. Alaloul, N. I. M. Yusoff, F. H. Khairuddin, et al. Evaluation of the high-temperature rheological performance of tire pyrolysis oil-modified bio-asphalt. *International Journal of Pavement Engineering*, 2021, pp. 1–16.
- [17] Liu, H., M. Zhang, Y. Wang, Z. Chen, and P. Hao. Rheological properties and modification mechanism of polyphosphoric acidmodified asphalt. *Road Materials and Pavement Design*, Vol. 21, No. 4, 2020, pp. 1078–1095.
- [18] Liu, Z., S. Li, and Y. Wang. Characteristics of asphalt modified by waste engine oil/polyphosphoric acid: Conventional, high-temperature rheological, and mechanism properties. *Journal of Cleaner Production*, Vol. 330, 2022, id. 129844.
- [19] Han, Y., J. Tian, J. Ding, L. Shu, and F. Ni. Evaluating the storage stability of SBR-modified asphalt binder containing polyphosphoric acid (PPA). Case Studies in Construction Materials, Vol. 17, 2022, id. e01214.
- [20] Liu, X., T. Li, and H. Zhang. Short-term aging resistance investigations of polymers and polyphosphoric acid modified asphalt binders under RTFOT aging process. *Construction and Building Materials*, Vol. 191, 2018, pp. 787–794.
- [21] Xu, S., H. Wu, W. Song, and Y. Zhan. Investigation of the aging behaviors of reclaimed asphalt. *Journal of Cleaner Production*, Vol. 356, 2022, id. 131837.
- [22] de Oliveira, Y. M. M., P. T. Cittadella, L. Rohde, and L. P. Thives. Simulation of the time needed for long-term asphalt ageing in the rolling thin film oven relative to that of the pressure ageing vessel. *Materials*, Vol. 16, No. 22, 2023, id. 7081.

DE GRUYTER

- [23] China, M. Standard test methods of bitumen and bituminous mixtures for highway engineering: JTG E20-2011, China Communications Press Beijing, China, 2011.
- [24] Sun, D. X., Y. Zou, H. Wang, and H. X. Weng. Study of road bitumen modified with heavy fraction of tire pyrolysis oil. *Energy Sources*, *Part A: Recovery, Utilization, and Environmental Effects*, Vol. 33, No. 19, 2011, pp. 1822–1831.
- [25] Lin, J., J. Hong, J. Liu, and S. Wu. Investigation on physical and chemical parameters to predict long-term aging of asphalt binder. *Construction and Building Materials*, Vol. 122, 2016, pp. 753–759.
- [26] Ding, Y., B. Huang, and X. Shu. Utilizing fluorescence microscopy for quantifying mobilization rate of aged asphalt binder. *Journal of Materials in Civil Engineering*, Vol. 29, No. 12, 2017, id. 04017243.
- [27] Zhou, T., L. Cao, E. H. Fini, L. Li, Z. Liu, and Z. Dong. Behaviors of asphalt under certain aging levels and effects of rejuvenation. *Construction and Building Materials*, Vol. 249, 2020, id. 118748.
- [28] Yang, C., J. Zhang, F. Yang, M. Cheng, Y. Wang, S. Amirkhanian, et al. Multi-scale performance evaluation and correlation analysis of blended asphalt and recycled asphalt mixtures incorporating high RAP content. *Journal of Cleaner Production*, Vol. 317, 2021, id. 128278
- [29] Xue, Y., C. Liu, S. Lv, D. Ge, Z. Ju, and G. Fan. Research on rheological properties of CNT-SBR modified asphalt. *Construction and Building Materials*, Vol. 361, 2022, id. 129587.
- [30] Liu, S., S. Zhou, and A. Peng. Evaluation of polyphosphoric acid on the performance of polymer modified asphalt binders. *Journal of Applied Polymer Science*, Vol. 137, No. 34, 2020, id. 48984.
- [31] Alam, S. and Z. Hossain. Changes in fractional compositions of PPA and SBS modified asphalt binders. *Construction and Building Materials*, Vol. 152, 2017, pp. 386–393.
- [32] McDaniel, R. S. and R. M. Anderson. Recommended use of reclaimed asphalt pavement in the Superpave mix design method: technician's manual, National Research Council (US). Transportation Research Board, Washington, DC, 2001.
- [33] Jiang, X., P. Li, Z. Ding, L. Yang, and J. Zhao. Investigations on viscosity and flow behavior of polyphosphoric acid (PPA) modified asphalt at high temperatures. *Construction and Building Materials*, Vol. 228, 2019, id. 116610.

- [34] Nan, H., Y. Sun, J. Chen, and M. Gong. Investigation of fatigue performance of asphalt binders containing SBS and CR through TS and LAS tests. *Construction and Building Materials*, Vol. 361, 2022, id. 129651.
- [35] Sun, Y., W. Wang, and J. Chen. Investigating impacts of warm-mix asphalt technologies and high reclaimed asphalt pavement binder content on rutting and fatigue performance of asphalt binder through MSCR and LAS tests. *Journal of Cleaner Production*, Vol. 219, 2019, pp. 879–893.
- [36] Zhang, H., K. Shen, G. Xu, J. Tong, R. Wang, D. Cai, et al. Fatigue resistance of aged asphalt binders: An investigation of different analytical methods in linear amplitude sweep test. *Construction and Building Materials*, Vol. 241, 2020, id. 118099.
- [37] Ge, D., K. Yan, L. You, and Z. Wang. Modification mechanism of asphalt modified with Sasobit and Polyphosphoric acid (PPA). Construction and Building Materials, Vol. 143, 2017, pp. 419–428.
- [38] Eniu, D., C. Gruian, E. Vanea, L. Patcas, and V. Simon. FTIR and EPR spectroscopic investigation of calcium-silicate glasses with iron and dysprosium. *Journal of Molecular Structure*, Vol. 1084, 2015, pp. 23–27.
- [39] Madejová, J., B. Arvaiová, and P. Komadel. FTIR spectroscopic characterization of thermally treated Cu²⁺, Cd²⁺, and Li⁺ montmorillonites. *Spectrochimica Acta, Part A: Molecular and Biomolecular Spectroscopy*, Vol. 55, No. 12, 1999, pp. 2467–2476.
- [40] Hou, X., S. Lv, Z. Chen, and F. Xiao. Applications of Fourier transform infrared spectroscopy technologies on asphalt materials. *Measurement*, Vol. 121, 2018, pp. 304–316.
- [41] Marsac, P., N. Piérard, L. Porot, W. Van den bergh, J. Grenfell, V. Mouillet, et al. Potential and limits of FTIR methods for reclaimed asphalt characterisation. *Materials and Structures*, Vol. 47, No. 8, 2014, pp. 1273–1286.
- [42] Campuzano, F., A. G. Abdul Jameel, W. Zhang, A. H. Emwas, A. F. Agudelo, J. D. Martínez, et al. On the distillation of waste tire pyrolysis oil: A structural characterization of the derived fractions. *Fuel*, Vol. 290, 2021, id. 120041.
- [43] Han, Y., B. Cui, J. Tian, J. Ding, F. Ni, and D. Lu. Evaluating the effects of styrene-butadiene rubber (SBR) and polyphosphoric acid (PPA) on asphalt adhesion performance. *Construction and Building Materials*, Vol. 321, 2022, id. 126028.